

Recent Development and Applications of Sensors for the Detection of Matrix Metalloproteinases

Huayue Zhang, Miaomiao Wu, Hang Thu Ta, Zhi Ping Xu, and Run Zhang*

Matrix metalloproteinases (MMPs) are a class of zinc-dependent endopeptidases that play important roles in disease progression. High expression of MMPs is associated with various diseases, including cancer, cardiovascular diseases, neurological diseases, and inflammatory diseases. For better understanding the roles of MMPs in these diseases' development and the potential in early diagnosis and treatment monitoring, a number of sensors have recently been developed for MMPs detection in vitro and in vivo. These sensors are designed mainly based on the exploration of MMPs' molecular structure and enzymatic activity. This review seeks to provide a summary for the development and application of the sensors for the detection of MMPs in the past three years. The research hotspots, current challenges, and further research directions in this field are also discussed.

1. Introduction

Matrix metalloproteinases (MMPs) are a class of zinc-dependent endopeptidases that were identified as early as 1962 by Gross in frog tail experiments.^[1] The main function of MMPs used to be considered to degrade extracellular matrix (ECM), the timely degradation of which is an important feature of normal cell development, morphogenesis, remodeling, and tissue repair.^[2] Historically, MMPs were divided into collagenases (MMP-1, MMP-8, MMP-13, and MMP-18), gelatinases (MMP-2 and MMP-9), stromelysins (MMP-3, MMP-10, and MMP-11), and matrilysins (MMP-7 and MMP-26) according to their specificity

of ECM cleavage. As the number of identified MMPs types increased, researchers began to classify the MMPs according to the protein structure.^[3] Despite some structural differences, most of the structural modules of MMPs are still conservative, including i) an amino-terminal peptide which can lead MMPs to the endoplasmic reticulum, ii) a propeptide region (companying with a zinc-interacting thiol group) and a zinc-binding site which can maintain MMPs as inactive zymogens or as a catalytic domain, iii) a linker region of varying residue length that may determine the substrates to which the MMPs can accommodate, and iv) a hemopexin-like domain.^[4]


With the application of engineered genetic models these years, more biological roles of MMPs have been revealed in recently years. For example, through investigating MMPs' substrates of other proteins, such as pro-proteases, chemokines, antimicrobial peptides, cell surface proteins, coagulation factors, adhesion molecules, cryptic growth factors, and cytokines,^[5] it has been revealed that the MMPs have a broad and dramatic impact on physiological processes, for example, immunity,^[6] tissue repair,^[7,8] cell differentiation,^[9,10] and cell invasion.^[11] In these physiological processes, MMPs are secreted as zymogens.^[12] The cysteine (Cys) residues of MMPs' propeptide regions are able to interact with Zn^{2+} of the catalytic domains. The formation of the thiols- Zn^{2+} bonds play important roles in maintaining the inactivity of MMPs, i.e., MMPs' activations are achieved by breaking these bonds. It is conceivable that MMPs can be activated by a variety of endogenous or exogenous substances, such as mercurial compounds and chaotropic agents.^[4] To regulate the activity of MMPs, organisms have evolved a family of two-domain proteins (TIMPs) as the endogenous inhibitors.^[13]

Most MMPs are ubiquitously secreted in mammalian organisms. The level of MMPs' expression is generally low under normal physiological conditions, while the abnormally elevated expression and activity levels are often associated with diseases. For example, as of the positive roles of MMPs in tumor growth and angiogenesis,^[14] recent studies revealed that MMPs overexpression is implicated in a variety of cancers.^[15] MMP-2 and MMP-9 are overexpressed in breast cancer,^[16] cervical cancer,^[17] etc., while MMP-7 are correlated with colorectal cancer (CRC).^[18] Moreover, the prognostic value of MMPs has also been well demonstrated in treatment of different cancers.^[19,20] For example, patients with high levels of MMP-2 and MMP-9 were clinically defined as a poor prognosis.^[21] Therefore, MMPs'

H. Zhang, M. Wu, H. T. Ta, Z. P. Xu, R. Zhang
Australian Institute for Bioengineering and Nanotechnology
The University of Queensland
Brisbane, QLD 4072, Australia
E-mail: r.zhang@uq.edu.au

H. T. Ta
School of Environment and Science
Griffith University
Brisbane, Queensland 4111, Australia

H. T. Ta
Queensland Micro- and Nanotechnology Centre
Griffith University
Nathan, QLD 4111, Australia

 The ORCID identification number(s) for the author(s) of this article can be found under <https://doi.org/10.1002/admt.202201786>.

© 2023 The Authors. Advanced Materials Technologies published by Wiley-VCH GmbH. This is an open access article under the terms of the Creative Commons Attribution-NonCommercial License, which permits use, distribution and reproduction in any medium, provided the original work is properly cited and is not used for commercial purposes.

DOI: 10.1002/admt.202201786

level has become the hallmark for the diagnosis and treatment monitoring of tumors' progression.^[22] In addition to tumors, the expression of MMPs is closely related to vascular diseases, such as atherosclerosis,^[23] hypertension,^[24] myocardial infarction (MI),^[25] and stroke.^[26] Similar to tumor, the association of vascular diseases with MMPs is mainly because of the MMPs-mediated remodeling of the ECM. It has been reported that the degradation of collagen and other ECM in the fibrous caps surrounding atherosclerotic plaques by MMPs may predispose the plaques to rupture.^[27] Moreover, the degradation activity of MMPs on non-ECM proteins such as cytokines, chemokines, and growth factors may also play an important role in the formation of atherothrombosis.^[28]

In recent years, the studies of the correlation between MMPs and neurological diseases have also received extensive attention and verification.^[29,30] Generally, MMPs are absent in the normal nervous system, while elevated MMP expression has been shown to correlate with neuroinflammation, nerve injury, and neurodegenerative diseases.^[31] MMPs lead to increased blood–brain barrier (BBB) permeability by attacking the ECM, substrates, and tight junctions of endothelial cells, resulting in acute neuroinjection inflammatory injury.^[32] Recent investigations have revealed that the MMPs are also implicated in inflammatory bowel diseases (IBDs),^[33] a worldwide inflammatory disease with increasing number of patients over the past 20 years.^[34] Although the etiology of the IBDs remains unclear, many studies have proposed the MMPs-mediated proteolytic regulation or regulation of transcription factors as risk factors for the development and progression of this disease.^[35] Studies have shown that the increase in MMPs levels in IBDs patients is not limited to the intestine, but also in saliva and serum.^[36] In addition to the diseases mentioned above, the level of MMPs is also inseparable from other inflammatory diseases such as periodontitis,^[37] arthritis,^[38] liver disease,^[39] bacterial and viral infections,^[40] and sepsis caused by infection.^[41] Although the protective effect of MMPs on diseases such as cancer and neurological diseases has also been confirmed under specific conditions,^[42,43] the roles of MMPs in these inflammatory disease remains unclear.

The development of reliable methods for the detection of MMPs in body is contributing significantly to obtaining new understandings the roles of MMPs in various diseases. In recent decades, in addition to the conventional techniques of zymography^[44,45] and enzyme-linked immunosorbent assay (ELISA),^[46] various sensors based on electrochemistry,^[47–49] fluorescence,^[50–55] surface-enhanced Raman scattering (SERS),^[56] etc., have been continuously developed for MMPs detection. The design of these MMPs sensors is generally based on the specific structure of these enzymes and their enzymatic activity. There have been reviews before 2019 summarized the methods for MMPs detection, focusing on the principles of the detection methods^[57] and the impact of nanomaterials.^[58] Undiminished research enthusiasm for MMPs investigations drives the development of new detection methods for these enzymes in the last three years. In this work, the development of sensors for MMPs detection in recent years, especially the past three years, is summarized (Table 1). The MMPs and their biological roles are introduced, followed by the summary of the sensors developed in last three years for MMPs detection. Corresponding

discussions mainly focus on the enzymes' structure- and the enzymatic activity-based sensors. This is followed by the concluding remarks to highlight the challenges in the field and propose the potential research directions in future.

2. MMPs Structure-Based Sensors

2.1. Antigen–Antibody Based Immunosensors

Immunosensor is a type of sensor that is developed based on the formation of stable immunocomplex through the specific immunoreaction between antibody and corresponding targeting antigen. Specifically, in animals, invasion of pathogens or other foreign proteins (antigens) triggers the production of antibodies that recognize and eliminate the antigens. The combination of antigen and antibody produces an immune response with extremely high selectivity and sensitivity.^[90] Based on this principle, numerous traditional methods, including immunohistochemistry (IHC),^[91] western blot (WB),^[92] and conventional ELISA^[93] have been established for the detection of MMPs. The mechanisms of these methods have been described systematically in previous reviews,^[51,94,95] so brief introduction of the immunosensors, particularly those of new advances, are included in this section.

IHC utilizes the specific binding between antigens and antibodies to determine the cellular antigens (polypeptides and proteins) using the antibodies that are labeled with the chromogenic reagents (e.g., fluorescein, enzymes, metal ions, isotopes). For the detection of MMPs in biological tissues, IHC is a straightforward, well-established, and robust technique due to the commercial availability of the large number of high-quality antibodies. For instance, in 2021, Broekaart et al. detected the expression level of MMPs by IHC and further investigated the antiseizure and antiepileptogenic effects of MMPs' endogenous inhibitor (IPR-179) in patients with status epilepticus (SE) or temporal lobe epilepsy (TLE) and in a rat temporal lobe epilepsy model.^[96] While this conventional technique is a popular approach to identify regions and cell types with increased expression of MMPs, IHC often cannot distinguish between latent and active proteases.

In short, the principle of WB is to separate and identify protein according to their molecular weight by polyacrylamide gel SDS-PAGE electrophoresis. The protein is transferred to a fixed carrier, such as polyvinylidene difluoride (PVDF) membrane, and is labeled with primary antibody and secondary antibody. The target protein is then determined by analyzing the size and color intensity of the protein band. For example, Miao et al. used WB to evaluate the expression of MMP-1, MMP-2, MMP-3, MMP-9, and MMP-13 while studying the effect of *Staphylococcus aureus* on the expression of bovine mammary fibroblasts MMPs/TIMPs and the uPA system.^[97] Although different forms of MMPs can be distinguished to some extent by the changes in molecular weight, considering dissociation, the small molecular weight band may not accurately represent endogenous activity.

Traditional ELISA is a comprehensive technology developed by organically combining the immune response of antigens and antibodies with the efficient catalytic reaction of

Table 1. Analytical performance of typical MMPs sensors.

Target	Sensing platform	Sensor type	Detection signal	Detection range	Detection limit	Ref.
MMP-9	MB	Immune-based	Electrochemical	8.0–75 pg mL ⁻¹	2.4 pg mL ⁻¹	[48]
MMP-1	AuNP/PEI/rGO	Immune-based	Electrochemical	1–50 ng mL ⁻¹	0.219 ng mL ⁻¹	[59]
MMP-9	Au/PAMAM-NH ₂ /Ab	Immune-based	Electrochemical	1 × 10 ⁻⁴ –5 μg mL ⁻¹	2.0 pg mL ⁻¹	[60]
MMP-7	CdTe/AgNP	Immune-based	Fluorescence	0.01–30 ng mL ⁻¹	7.3 pg mL ⁻¹	[61]
MMP-8/MMP-9	Magnetic and fluorescent beads	Immune-based	Fluorescence	0.47–30 ng mL ⁻¹	0.24/0.38 ng mL ⁻¹	[62]
MMP-2	Au/PEI/Gly-Leu-AQ	Immune-based	Electrogravimetric	2–5 pg mL ⁻¹	10 fg mL ⁻¹	[63]
MMP-8	Biochip	Immune-based	SAW	0–1000 ng mL ⁻¹	62.5 ng mL ⁻¹	[64]
MMP-9/MMP-2	PDNAS	DNA aptamer-based	Fluorescence	24–600/64–1600 pg mL ⁻¹	9.6/25.6 pg mL ⁻¹	[65]
MMP-9	AuNS	DNA aptamer-based	PA	–	–	[66]
MMP-12	Hydroxamate	Inhibitor-based sensors	Radiochemical	–	–	[67]
MMP-1	MIP	MIPs-based	Electrochemical	50–500 × 10 ⁻⁹ M	20 × 10 ⁻⁹ M	[68]
MMP-2	PANI gel/CS-AuNPs-Pb ²⁺	Enzymatic activity-based	Electrochemical	1 pg mL ⁻¹ to 1 μg mL ⁻¹	0.4 pg mL ⁻¹	[69]
MMP-2	MSFs/[Ru(NH ₃) ₆]Cl ₃	Enzymatic activity-based	Electrochemical	0.01–20 ng mL ⁻¹	0.98 ng mL ⁻¹	[70]
MMP-2	PAA	Enzymatic activity-based	Electrochemical	0.625–20 ng mL ⁻¹	6.6 fg mL ⁻¹	[71]
MMP-2	Graft ferrocene polymer	Enzymatic activity-based	Electrochemical	1 pg mL ⁻¹ to 1 ng mL ⁻¹	0.27 pg mL ⁻¹	[72]
MMP-2	NGQDs-Ru@SiO ₂	Enzymatic activity-based	ECL	0.01–185 ng mL ⁻¹	6.5 pg mL ⁻¹	[73]
MMP-2	g-C ₃ N ₄ /AuNP	Enzymatic activity-based	PEC	1 pg mL ⁻¹ to 100 ng mL ⁻¹	0.55 pg mL ⁻¹	[74]
MMP-9	GO-Pep-Pdot	Enzymatic activity-based	Fluorescence	10–110 ng mL ⁻¹	3.75 ng mL ⁻¹	[75]
MMP-2	MP/NPs-SLIPS	Enzymatic activity-based	Fluorescence	–	3.7 ng mL ⁻¹	[76]
MMP-2/MMP-7	DNA-peptide conjugates	Enzymatic activity-based	Fluorescence	3.80–1200 × 10 ⁻¹² M/ 1.80–572 × 10 ⁻¹² M	3.33 × 10 ⁻¹² M/1.71 × 10 ⁻¹² M	[77]
MMP-2	T7 RNA polymerase	Enzymatic activity-based	Fluorescence	0.3 × 10 ⁻¹² M to 7.0 × 10 ⁻⁹ M	0.07 × 10 ⁻¹² M	[78]
MMP-7	FITC/RhB/MnFe ₂ O ₄	Enzymatic activity-based	Fluorescence	0.1–15 × 10 ⁻⁹ M	0.1 × 10 ⁻⁹ M	[79]
MMP-2	SPN-MMP-RGD	Enzymatic activity-based	Fluorescence	0.05–1 × 10 ⁻⁹ M	0.036 × 10 ⁻⁹ M	[80]
MMP-2	UCNPs-Cy3/Pep-QSY7/Ab	Enzymatic activity-based	Fluorescence	1–100 ng mL ⁻¹	0.51 ng mL ⁻¹	[81]
MMP-2	7-HC-CL	Enzymatic activity-based	CL	–	–	[82]
MMP-2	Cy5.5/QSY21	Enzymatic activity-based	PA	0–320 ng mL ⁻¹	0.52 ng mL ⁻¹	[83]
MMP-2	AuNP/RhB/2-NT	Enzymatic activity-based	SERS	8–400 ng mL ⁻¹	–	[84]
MMP-2	Peptide/Isotope	Enzymatic activity-based	MS	–	10 ng mL ⁻¹	[85]
MMP-2/MMP-7	Ni-NTA MBs/ Isobaric tags	Enzymatic activity-based	MS	0.2–100/0.5–400 ng mL ⁻¹	0.0064/0.17 ng mL ⁻¹	[86]
MMP-2	MMP-Fe/IONPs	Enzymatic activity-based	MRI	–	–	[87]
MMP-2	FMNS@Au	Dual-mode signal sensor	Fluorescence/SERS	1–200 ng mL ⁻¹	0.35 ng mL ⁻¹	[88]
MMP-2	MBS-peptide (-FAM)-AuNP	Dual-mode signal sensor	MS/Fluorescence	0.05–50 ng mL ⁻¹	0.02 ng mL ⁻¹	[89]

enzymes. Through immobilization of antigen (antibody) on the solid phage carrier, the target analyte is able to be detected by analyzing the color depth of the complex containing enzyme-labeled antigen (antibody), solid-phased antigen-antibody, and the substrate solution. By selecting antibodies against different MMP domains, a highly accurate method for the determination of MMP protein levels can be achieved.^[98] As an example, Jansen et al. measured the concentrations of MMP-1 and MMP-9 using commercially available ELISA kits to investigate the role of MMPs in the pathogenesis of chronic Q fever.^[99] Although some advantages of ELISA for MMPs analysis, the sensitivity of this colorimetric method is not satisfied. Moreover, the practical application of this ELISA approach is also limited due to the cumbersome separation, washing process, and high cost of antibodies.

2.1.1. Electrochemical Sensors

Electrochemical sensors use electrodes as conversion elements and immobilized carriers, to immobilize biologically sensitive substances, such as antigens, antibodies, enzymes, and hormones, or organisms themselves as sensitive elements on the electrodes. Through the specific recognition between biomolecules, the target molecule and its reaction signal are converted into electrical signals that are recorded for the detection of target analyte. The detection of targets by electrochemical immune sensors is normally based on the analytical response and signal amplification after the formation of immune complexes. As of the advantages including high sensitivity, good selectivity, wide linear range and low detection limit, as well as general low cost and ease of use, various electrochemical

techniques including, for example, voltammetry,^[100,101] electrochemical Impedance (EIS),^[102–104] electrochemiluminescence (ECL),^[105] and field effect transistor (FET)^[106,107] have recently been used to design sensors for the detection of MMPs.

There are two main strategies, including sandwich-type and label-free for the design of electrochemical immunosensors for MMPs.^[108] Sandwich-type (labeled) immunosensors generate electrochemical signals through redox probes or enzyme-labeled secondary antibodies. In 2021, Arévalo et al. reported a sandwich-type immunoassay for the amperometric determination of MMP-9 on screen-printed carbon electrodes (SPCEs).^[48] The capture antibody (cAb) on a magnetic microbeads was used to capture MMP-9, followed by the formation of the sandwich biotinylated detector antibody (biotin-dAb)-streptavidin-horse radish peroxidase (Strep-HRP) complex (Figure 1). The MMP-9 detection was then achieved by amperometric analysis of HRP-H₂O₂/hydroquinone (HQ) system. This sandwich-type sensor exhibited high sensitivity with limit of detection (LoD) 2.4 pg mL⁻¹ for MMP-9 detection.

Due to the short fabrication time with reduced chemical consumption and low cost,^[109] the development of label-free immunosensor for MMPs detection has attracted enormous attention in recent years.^[110] For example, Yaiwong et al. reported a label-free immunosensor for electrochemical detection of MMP-7 in sera.^[111] In this immunosensor system, 2D molybdenum disulfide (2D MoS₂)/graphene oxide (GO) nanocomposite on a SPCE offered large specific surface area, fast electron transfer, and exceptional electrical conductivity for MMP-7 detection. The anti-MMP-7 capture antibodies on the surface of nanocomposite used to recognize the MMP-7 immunocomplex and methylene blue (MB) was co-loaded on the surface for the amplification of electrochemical signal. This sensor enabled detection of MMP-7 in the range of 0.010–75 ng mL⁻¹ with a LoD of 0.007 ng mL⁻¹. Similar design of the immunosensor has been described by Liu et al. in 2021. The MMP-1 immunosensor was prepared based on the modification of gold nanoparticles (NPs)/polyethyleneimine/reduced graphene oxide (AuNP/PEI/RGO). The sensor finally showed good detection capability in the linear range of 1–50 ng mL⁻¹ with an LoD of 0.219 ng mL⁻¹ (Figure 2a).^[59]

In addition to the signal amplification for target analytes detection, the selection of an appropriate linker for immobilizing receptors on the selected substrates is also an effective approach for further improving the sensitivity of the detection. To improve the linkers' immobilization efficiency, accessibility, and receptors' distribution on 2D materials, Nisiewicz et al.

designed a immunosensor using 3D dendrimer scaffolds as linkers for the detection of total MMP-9 in plasma (Figure 2b).^[60] The G2 poly(amidoamine) dendrimer (PAMAM)-based 3D platform expanded the surface area of the receipt layer, thus improved the sensitivity for MMP-9 detection. It was found that the functional groups of PAMMA (i.e., PAMAM-NH₂ and PAMAM-COOH) could contribute to the orientation of the antibody molecules on the substrate surface. The results showed that the PAMAM-NH₂ based immunosensor has higher sensitivity (LoD 2 pg mL⁻¹) and wider detection range (1 × 10⁻⁴–5 mg mL⁻¹) in comparison with PAMAM-COOH based immunosensor. Using this immunosensor, determination the level of MMP-9 in commercial human and rat plasma was successfully demonstrated.

FET-based devices have also been demonstrated as promising electrochemical sensors for ultrasensitive, real-time, multiplexed, and label-free detection of molecular species in a wide range of applications. For example, Lu et al. developed a uniform and stable silicon nanowire-based (SiNW) FET using an improved controllable process to detect MMP-9 levels in standard and human tear samples.^[112] The antibody was attached to SiNW through a -CHO and -NH₂ reaction, and was used to capture MMP-9 in tear samples. The use of these SiNW devices was demonstrated for the detection of dry eye with human tear samples.

2.1.2. Fluorescence Sensor

Fluorescent immunosensors using specific antigen-antibody recognition has also been developed for MMPs detection in recent years. Fluorescent proteins,^[113] fluorescent dyes,^[114,115] quantum dot labels,^[116,117] etc., have been explored as the signaling unit for the design of fluorescence sensors. In comparison with other analytical techniques, MMPs analyses using fluorescence sensors are featured with multicolor labeling ability, low cost, high sensitivity, and signal intensity, and thus has attracted widespread attention for rapid detection and imaging of MMPs in vitro and in vivo.^[118]

In 2020, Huang et al. demonstrated a paper-based visual fluorescence immunoassay to detect MMP-7 (Figure 3a).^[61] After a sandwich-type immunoreaction between silver nanoparticle (AgNP)-labeled secondary antibody/primary antibody-coated microtiter wells and MMP-7, the AgNP was dissolved with HNO₃ to form the free Ag⁺ ions. The Ag⁺ ions were then interacted with CdTe QDs through an ion-exchange reaction

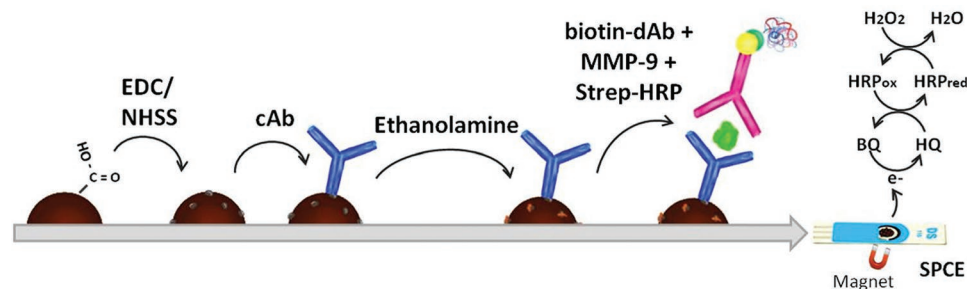


Figure 1. A representative sandwich-type immunosensor for MMPs detection. Procedure of the MMPs immunosensor fabrication and the principles for the detection. Determination of MMP-9 at a SPCE was achieved with an HQ system. Reproduced with permission.^[48] Copyright 2021, Elsevier.

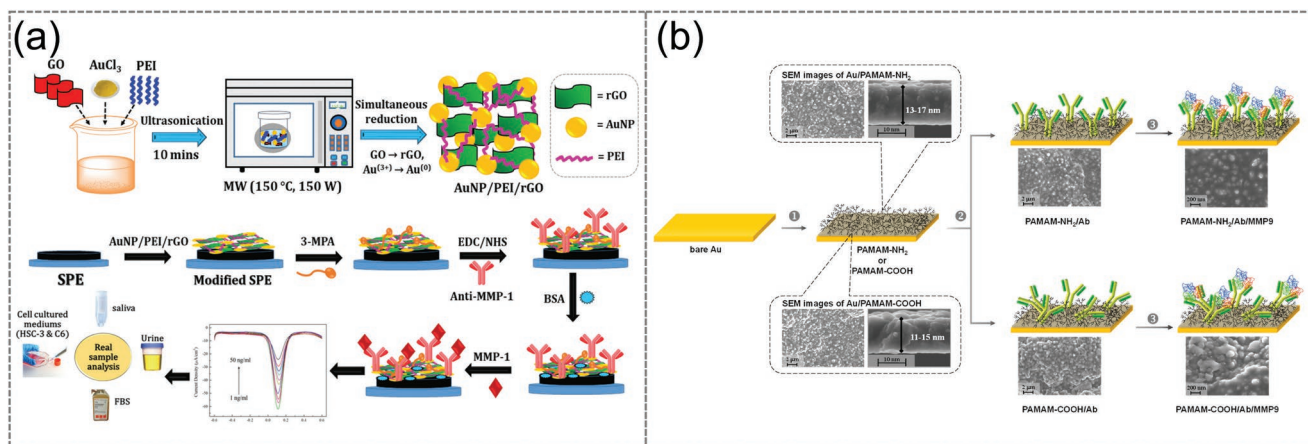


Figure 2. Label-free electrochemical immunosensor for MMPs detection. a) MMP-1 immunosensor based on the modification of AuNP/PEI/RGO. Reproduced with permission.^[59] Copyright 2021, The Royal Society of Chemistry. b) MMP-9 immunosensor using 3D dendrimer scaffolds as linkers. Reproduced with permission.^[60] Copyright 2022, Elsevier.

to quench the QDs' emission. This sensor featured with high sensitivity ($\text{LoD } 7.3 \text{ pg mL}^{-1}$) and accuracy (variation coefficients $<6.9\%$ and 12.4% for intra-assay and inter-assay, respectively). In another work, Johannsen et al. reported a competitive, one-step, double-bead, no-wash, heterogeneous immunoassay method for the detection of MMP-8 and MMP-9 (Figure 3b).^[62] In this method, magnetic beads were used as the capture agents and fluorescent beads were used as the detection agents. This method retained the advantages of ELISA and bead-based assays while adding key features of fast, elution-free operation, untethered phase detection, and simplified multiplexing capabilities.

2.1.3. Other Signals-Based Sensors

In addition to the electrochemical and fluorescence sensors, other signals-based sensors, including electrogravimetric and surface acoustic wave (SAW) sensors have also been recently developed for MMPs detection. Electrogravimetric sensors are one kind of effective methods for specific antigen detection. The basic principle of this method is to bind the target analytes through antigen–antibody recognition, and then record the quality of each layer of the immunosensor on the electrode surface. Based on this principle, Nisiewicz et al. developed an electrogravimetric sensor for the detection of MMP-2 in 2022.^[63] The sensor was fabricated by first attaching cationic polymer (PEI) to the surface of Au disc electrode, and then conjugating with antibody through EDC-NHS chemistry or immobilization of the anthraquinone (AQ) dipeptide. The sensor exhibited wide detection range ($2\text{--}5 \text{ pg mL}^{-1}$) and high sensitivity ($\text{LoD } 10 \text{ fg mL}^{-1}$). The application of the sensor for MMP-2 detection in blood plasma was then demonstrated.

SAW sensors are new type of microacoustic sensors that use SAW devices as sensing elements. In the SAW device, the change of the speed or frequency of the SAW is tested and then the signal is converted to electrical signal output as the measurement result. Taylor et al. described a biosensor that captures MMP-8 using specific antibodies coated on a small biochip and then analyzed the salivary MMP-8 by microelectromechanical

piezoelectric SAW technology. This sensor was then demonstrated to differentiate periodontitis from gingivitis and track the changes of MMP-8 after clinical treatment.^[64]

2.2. Aptamer-Based Sensors

In addition to the above outlined antigen–antibody binding, recent advances of the sensors' development involve the use of DNA aptamer as the sensing unit for MMPs detection. Upon specific stimuli, such as pH or biomolecules, the structure of oligomeric DNA sequences is changed, resulting in the inhibition the formation of sequence-specific duplexes with their complementary sequences. DNA aptamers, oligonucleotides that bind to specific target molecules, represent a class of functional oligomeric DNA sequences.^[119,120] The sensors developed using the DNA hybridization instead of antibody binding to MMPs have the advantage of being programmable, predictable, and biocompatible.

In 2020, Yu et al. reported the fabrication of the polydopamine nanospheres (PDANS)-based nanoplatfor for simultaneous detection of MMP-9 and MMP-2 (Figure 4a).^[65] In this sensor, the 5'-FAM (5-carboxyfluorescein) labeled MMP-9 aptamer and Texas Red labeled MMP-2 aptamer were loaded on the surface of PDNAS through $\pi\text{--}\pi$ deposition and hydrogen bond. The emission of both 5'-FAM and Texas Red were quenched due to the Förster resonance energy transfer (FRET) from fluorophores to PDANS. In the presence of MMP-9 and MMP-2, aptamers can specifically bind to the corresponding targets to form aptamer/target complexes, resulting in the release of aptamers from the surface of PDANS and thus the fluorescence recovery. The selective hydrolysis of aptamers triggered the release of the target, which induced a new round of fluorescence recovery for the amplification of fluorescence signal. This method was then used for MMPs detection in both urine and tissue homogenates of mice with unilateral ureteral obstruction (UUO).

Recently, Kim et al. designed DNA aptamer-gold nanospheres (AuNSs)-based sensor for photoacoustic (PA) detection

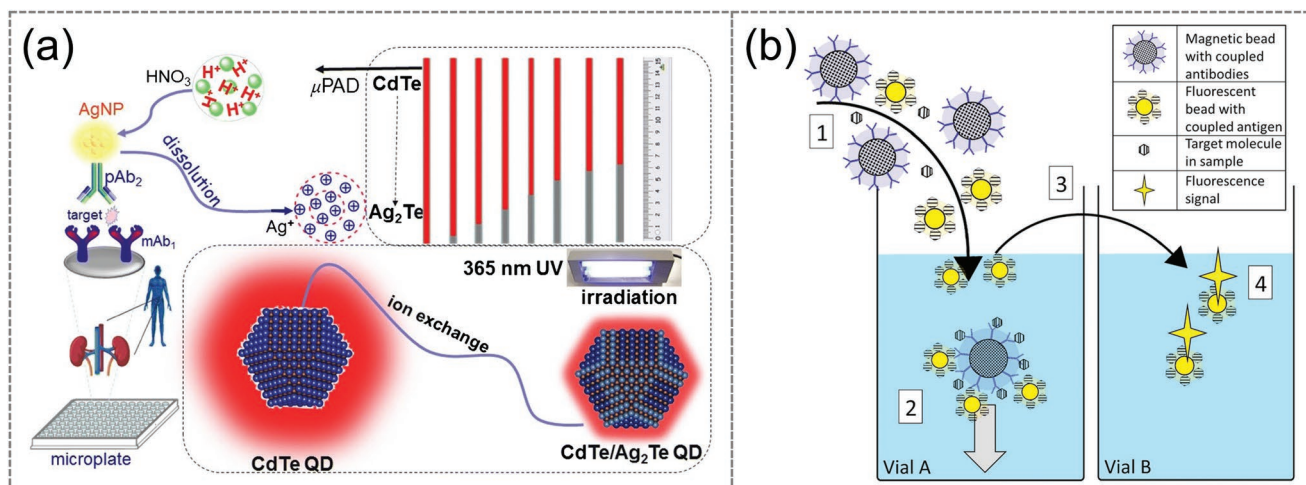


Figure 3. Immuno-based fluorescent sensors for MMPs. a) A paper-based visual MMP-7 fluorescence immunoassay. Reproduced with permission.^[61] Copyright 2020, Springer. b) A bound-free phase detection (BFPD) assay for the detection of MMP-8 and MMP-9. Reproduced with permission.^[62] Copyright 2021, Elsevier.

and imaging of MMP-9. In this PA sensor, the surface of AuNS-1 was modified with the double-stranded DNA aptamer and its complementary sequence (comp-1), and surface of AuNS-2 was modified with single stranded, full matched complementary sequences of comp-1 (comp-2) (Figure 4b).^[66] After combining DNA aptamers and plasmonic gold nanospheres, the nanospheres tend to aggregate in the presence of MMP-9 through DNA replacement and hybridization. Such an aggregation led to the emergence of new absorption at about 700 nm that was then used as a new PA signal for the detection of MMP-9. Detection of MMP-9 *in vitro*, *in cell culture*, and *in vivo* was then demonstrated.

2.3. Inhibitor-Based Sensors

It has been reported that the inhibitor-based sensors selectively bind to the active form of MMPs.^[102] Over the years, due to the negative effects of MMPs in various diseases, many researchers

have devoted themselves to the study of highly selective inhibitors against MMPs.^[121] The binding capacity and specificity requirements of inhibitors make them a potential antibody surrogate. For example, Gona et al. reported the development of a selective inhibitor of MMP-12 by introducing an acid around the P3'-segment of succinyl hydroxamate analogues and combining it with a radiotracer for tracking MMP-12 that highly expressed in abdominal aortic aneurysms.^[67] Although these inhibitor-based tracers have the advantage of being more stable compared to natural antibodies, *in vivo* studies showed nonspecific interaction of these probes with serum albumin.

2.4. Molecularly Imprinted Polymers (MIPs)-Based Sensors

MIPs are cost-effective and durable materials that can be used to replace natural antibodies.^[122] Molecular imprinting of proteins usually uses target protein as a template to imprint the protein, and then remove the protein molecule from the MIPs

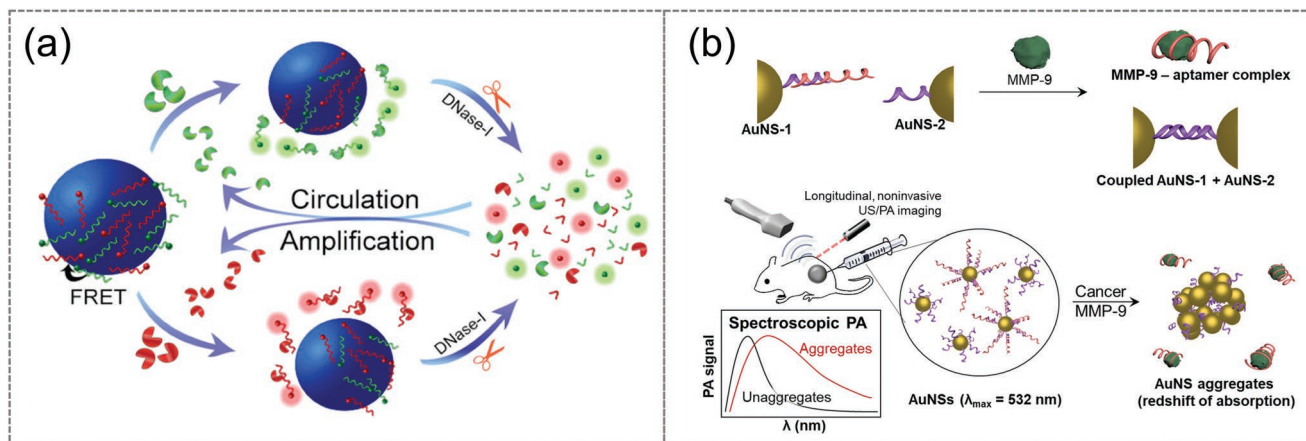


Figure 4. DNA aptamer-based sensors for MMPs. a) A polydopamine nanospheres (PDANS)-based nanoplatform for simultaneous detection of MMP-9 and MMP-2.^[65] Copyright 2020, American Chemical Society. b) A DNA aptamer-gold nanospheres (AuNSs) based sensor for PA detection and imaging of MMP-9. Reproduced with permission.^[66] Copyright 2022, Elsevier.

body. The resulting polymer is called MIPs that are used to recognize the protein.^[123] Considering the instability of biological components in the sensor, Bartold et al. developed a conductive MIPs film for MMP-1 detection. The MIPs sensor was prepared by extracting the template with 0.5×10^{-3} M triethylamine or a mixture of 10×10^{-3} M triethylamine and 5% ethanol of the volume ratio 1:1. Ultimately, MMP-1 detection in the range of $50\text{--}500 \times 10^{-9}$ M within human serum was achieved using this MIP sensor.^[68]

3. Enzymatic Activity-Based Sensors

As one type of enzymes, MMPs-triggered enzymatic cleavage reactions have also been explored as the mechanism for the design of sensors for MMPs detection. In fact, zymography is the most widely used as a mature cleavage-based method for the detection of MMPs in SDS-PAGE electrophoresis and reversed-phase gel staining protocol. Nevertheless, this method is not able to detect all MMPs in the practical sample, and most importantly, cannot distinguish different kinds of MMPs. In following research, peptides that are specifically cleaved by various types of MMPs are used in the development of sensors. The development of peptide cleavage-based probes is directly inspired by the peptide sequences of natural MMP substrates, or from combinatorial libraries of peptides obtained by phage display or chemical methods. Compared with the above MMPs' structure-based sensors, cleavage-based sensors can detect the activity of MMPs more directly and accurately. For example, GPLGVRGY is a peptide sensitive to MMP-2 as it can be cleaved into two fragments. Similarly, MMP-9 can selectively digest the GGKGPLGLPG peptide into two peptides, GGKGPL and GLPG. The ease of modification of peptides makes the design of enzyme cleavage-based sensors more flexible than structure-based methods and thus has gained more attention in recent years.^[124] In the following section, the use of enzymatic cleavage of peptides in the design of MMPs sensors, including electrochemical, ECL, photoelectrochemical (PEC), fluorescence, chemiluminescence (CL), PA, SERS, mass spectrometry (MS), and magnetic resonance imaging (MRI) sensors are discussed.

3.1. Electrochemical Sensors

3.1.1. Traditional Electrochemical Sensors

Peptide cleavage-based electrochemical sensors for the detection of MMPs have become one of the research focuses on recent studies. Taking advantage of the excellent conductivity and large specific surface area of polyaniline (PANI) gels, as well as the ability of CS-AuNPs-Pb²⁺ to significantly improve the interface resistance, Wang et al. developed an amperometric biosensor for MMP-2 detection. The sensor was fabricated using polyaniline gel as a substrate and Pb²⁺ supported carbon spheres (CS)-gold nanoparticle nanocomposites (CS-AuNPs-Pb²⁺) as a impedance enhancer (Figure 5a).^[69] The cleavage of the peptide led to the release of the CS-AuNPs-Pb²⁺ to change the square wave voltammetry (SWV) signals that was further

enhanced by the addition of sodium tartrate. The sensor was featured with a detection range of 1 pg mL^{-1} to $1 \text{ } \mu\text{g mL}^{-1}$ and a LoD of 0.4 pg mL^{-1} for MMP-2 analysis.

Based on ordered distribution of mesoporous silica thin films (MSFs) modifications, Duan et al. reported an electrode strategy for monitoring matrix metalloproteinase 2 (MMP-2) activity in 2021 (Figure 5b).^[70] MSFs are a type of solid-state nanofilm with adjustable nanopores and the ability to intelligently control molecular transport, such as the loading of $[\text{Ru}(\text{NH}_3)_6]\text{Cl}_3$. The positively charged substrate peptide on the negatively charged MSFs prevented the diffusion of $[\text{Ru}(\text{NH}_3)_6]\text{Cl}_3$, while after a MMP-2 initialized cleavage of the substrate peptide, the short segments could no longer block the $[\text{Ru}(\text{NH}_3)_6]\text{Cl}_3$'s diffusion, allowing higher DPV electrochemical signals for MMP-2 detection. The sensor developed in this work effectively inhibits the interference of coexisting substances through the antifouling ability and the molecular sieve effect of MSFs, making the signal more stable and suitable for MMP-2 detection in complex samples. In another work, Wang et al. proposed a strategy to monitor MMP-2 by assembling peptide scaffolds on ion nanochannels (Figure 5c).^[71] The self-assembly of the peptide on the porous anodic alumina (PAA) inhibited the ion current rectification (ICR), while the MMP-2 could cleave the peptide to increase the ICR effect. This method with 0.625 to 20 ng mL^{-1} detection range and 6.6 fg mL^{-1} LoD was then used for MMP-2 detection in tumor microenvironment.

As discussed above, signal amplification has been known as an effective approach for improving sensitivity for targeted analyte's detection. Taking this fact in consideration, Hu et al. developed a cleavage-based electrochemical sensor for MMP-2 detection (Figure 5d).^[72] Recognition peptides with a Cys residue at the N-terminus were immobilized by a chemical reaction of mature gold-sulfur self-assembly. Specific cleavage of the recognition peptide by MMP-2 produced a free carboxyl group at the C-terminus of the remaining fragment, and CPADs was then attached via a Zr(IV) linker. After that, a large number of Fc redox reporters were recruited on the electrode surface by electrochemically induced reversible addition-fragmentation chain-transfer (eRAFT) polymerization to graft ferrocene polymer to achieve signal amplification. Thereby lower detection limit (0.27 pg mL^{-1} with the detection range from 1 pg mL^{-1} to 1 ng mL^{-1}) for MMP-2 detection was obtained using this method.

3.1.2. ECL Sensors

In the past few decades, ECL has achieved great success with its simple device, near-zero background, good electrochemical performance, and excellent sensitivity.^[125] In 2021, Fan et al. developed a sensitive biosensor for MMP-2 determination using an $\text{Ru}(\text{bpy})_3^{2+}$ loaded N-GQDs and silica nanoparticle (NGQDs-Ru@SiO₂) as a luminophore and a MMP-2 cleavable peptide as a recognition element (Figure 6a).^[73] In this ECL sensor, NGQDs-Ru@SiO₂ served as a co-reactant of $\text{Ru}(\text{bpy})_3^{2+}$, which exhibited strong ECL performance due to the short distance between the luminophore and the co-reactant. The NGQDs-Ru@SiO₂ was then immobilized on the gold electrode surface by the Au-S bond. In the presence of the target molecule

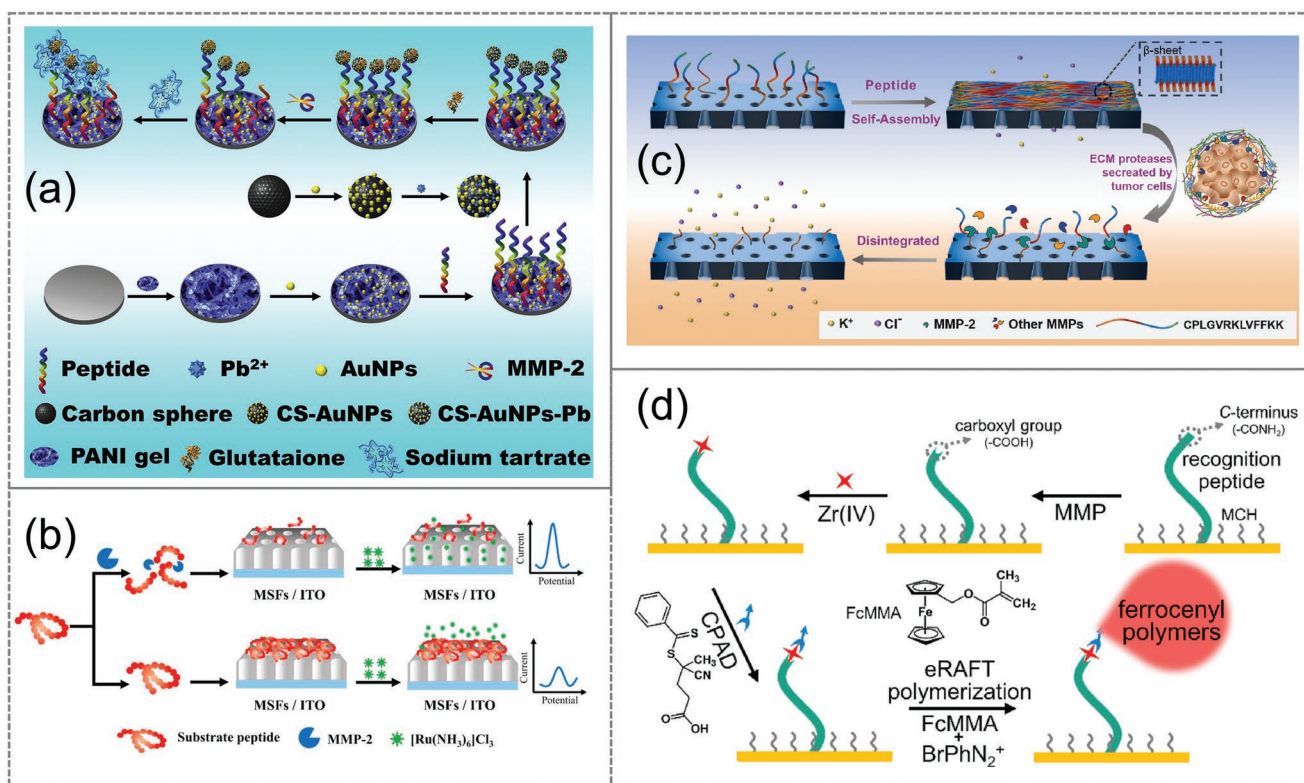


Figure 5. Representative design ideas of electrochemical sensors based on enzyme cleavage. a) An amperometric biosensor based on Pb²⁺ supported CS-gold nanoparticle nanocomposites for MMP-2 detection. Reproduced with permission.^[69] Copyright 2019, Elsevier. b) An electrode strategy based on ordered distribution of mesoporous silica thin films (MSFs) modifications for MMP-2 activity monitoring. Reproduced with permission.^[70] Copyright 2021, Elsevier. c) A strategy based on peptide scaffolds and ion nanochannels for MMP-2 monitoring.^[71] Copyright 2022, Elsevier. d) A MMP sensor based on electrochemically induced grafting of ferrocenyl polymers. Reproduced with permission.^[72] Copyright 2021, Elsevier.

MMP-2, part of the peptide-NGQDs-Ru@SiO₂ was detached from the electrode surface, resulting in the decrease of the ECL signal. The sensor showed a high sensitivity with LoD 6.5 pg mL⁻¹. The application of this sensor for MMP-2 detection in clinical serum samples was demonstrated, showing 91.5%–109.0% recovery and 2.7%–5.9% RSD.

3.1.3. PEC Sensors

PEC analysis relies on the electrochemical process of light signal, has emerged as a promising analytical method for bio-sensing. The sensing principle relies on charge separation and subsequent charge transfer after photoexcitation of photoactive

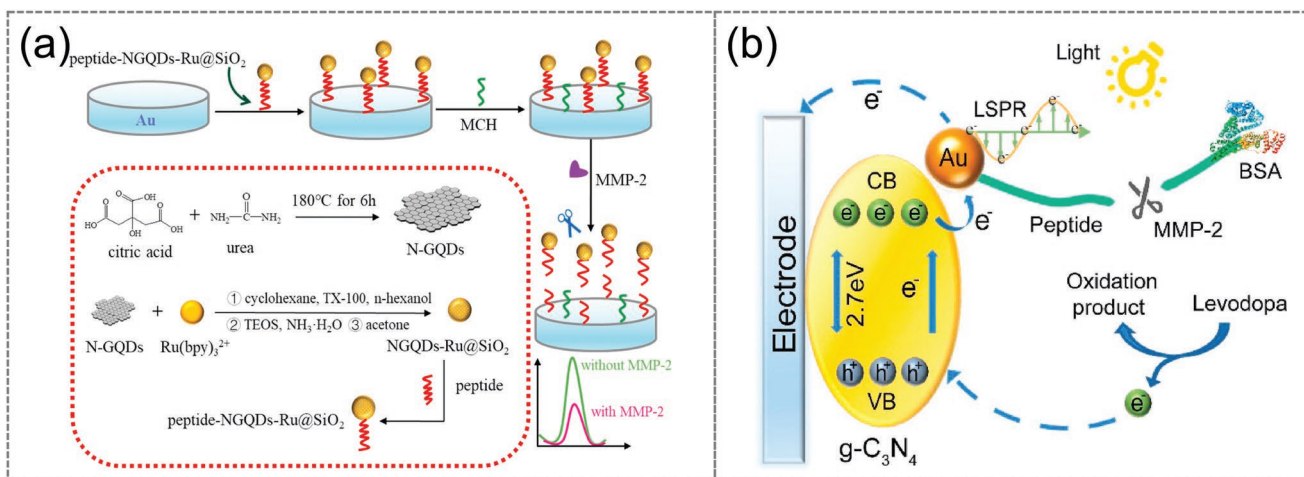


Figure 6. a) A MMP-2 ECL biosensor based on Ru(bpy)₃²⁺ loaded N-GQDs and silica nanoparticle (NGQDs-Ru@SiO₂) Reproduced with permission.^[73] Copyright 2021, Elsevier. b) A smartphone-based PEC biosensing system for MMP-2 detection. Reproduced with permission.^[74] Copyright 2021, Elsevier.

materials, and thus the photoactive materials are the key components of the PEC analysis. For MMPs analysis, Zhang et al. developed a smartphone-based PEC biosensing system in 2021 for MMP-2 detection (Figure 6b).^[74] The sensor was fabricated by using g-C₃N₄ as the photoactive material, while the gold nanoparticles as the signal amplification element and the carrier for immobilizing the MMP-2-specific cleavage peptide. In the presence of MMP-2, part of the peptide chain was separated from the electrode, resulting in the decrease in steric hindrance and an increase in PEC current. This method showed a detection range and LoD 1 pg mL⁻¹ to 100 ng mL⁻¹ and 0.55 pg mL⁻¹ for MMP-2 detection in serum, respectively.

3.2. Optical Sensors

3.2.1. Fluorescence Sensors

As highlighted above, fluorescence has become one of the preferred signals when designing sensors due to the advantages of high sensitivity, real-time monitoring, fast imaging speed, and low cost.^[126–129] Generally, the sensors are designed by linking the fluorophores to peptides that are sensitive to a specific enzyme, and the release of fluorophore with corresponding fluorescence response is obtained after a specific enzymatic cleavage reaction. On the basis of this strategy, a variety of fluorescent sensors based on the enzymatic cleavage mechanism has been developed in recent years for the detection of MMPs, which are summarized in this section.

In 2019, Li et al. assembled the peptide-linked polymer dots (Pdots) on the surface of graphene oxide to construct a graphene oxide-peptide-polymer dot (GO-Pep-Pdot) nanocomposite for the detection of MMP-9 (Figure 7a).^[75] In this sensors, the fluorescent Pdots that are obtained by crosslinking linear polymers or monomers under mild conditions was conjugated with peptides through the EDC–NHS based crosslinking. The attachment of the Pep-Pdot to GO quenched it's the emission through a FRET principle. As the MMP-9 triggered the cleavage of the peptide to release free GO and Pdots, the fluorescence is switched “on”, and the fluorescence intensity is correlated to

the activity of the MMP-9. This fluorescent sensor is sensitive to MMP-9 with a LoD 3.75 ng mL⁻¹, allowing it to be further applied to detect MMP-9 in prostate cancer clinical serum samples. Taking the advantages of aggregation-induced emission (AIE),^[130,131] Wu et al. designed a turn on fluorescent sensor (MP/NPs-SLIPS) for MMP-2 detection (Figure 7b).^[76] The MP/NPs-SLIPS sensing system consists of three components, including the MMP-2 cleavable MP probe, negatively charged NPs, and slippery lubricant-infused porous substrates (SLIPS). In the presence of MMP-2, the cleavage of the hydrophilic peptide chain led to the release of the AIEgens that was then aggregated with the assistance of negatively charged NPs, resulting in enhancement of the fluorescence for MMP-2 detection. This sensing system with high sensitivity (LoD 3.7 ng mL⁻¹) for MMP-2 is potentially used for the detection of MMP-2 secretion in cancer cells.

Amplification of fluorescence signal is an effective method for improving the sensitivity for the detection of target analytes. Through combining protease-sensitive cleavage with nickase-assisted signal amplification (NESA), Li et al. constructed a sensitive protease sensor for the detection of MMP-2 and MMP-7 in 2020 (Figure 8a).^[77] This sensor included two DNA–peptide conjugates containing specific protease cleavage sites, trigger DNA to convert the signal from MMPs, and two report DNAs that are labeled with Cy3 and Cy5 fluorophores and a BHQ2 quencher. Trigger DNA can hybridize with the corresponding reporter DNA to initiate a cyclic NESA reaction for signal amplification, releasing a large amount of Cy3/Cy5 fluorescent molecules for MMPs detection. The protease sensor can simultaneously respond MMP-2 and MMP-7 with LoD 3.33 and 1.71 × 10⁻¹² M, respectively. The applications of this sensor for MMP-2 and MMP-7 detection in cancer cells and the protease inhibitors' screening were demonstrated successfully. In the same year, Liu et al.^[78] and Luo et al.^[132] successively proposed transcription process-based signal amplifiers for the development of sensors for fluorescence detection of MMP-2. In this sensor system, activation of T7 RNA polymerase by protease was explored to amplify proteolysis into nucleic acid signal output for MMP-2 detection (Figure 8b).

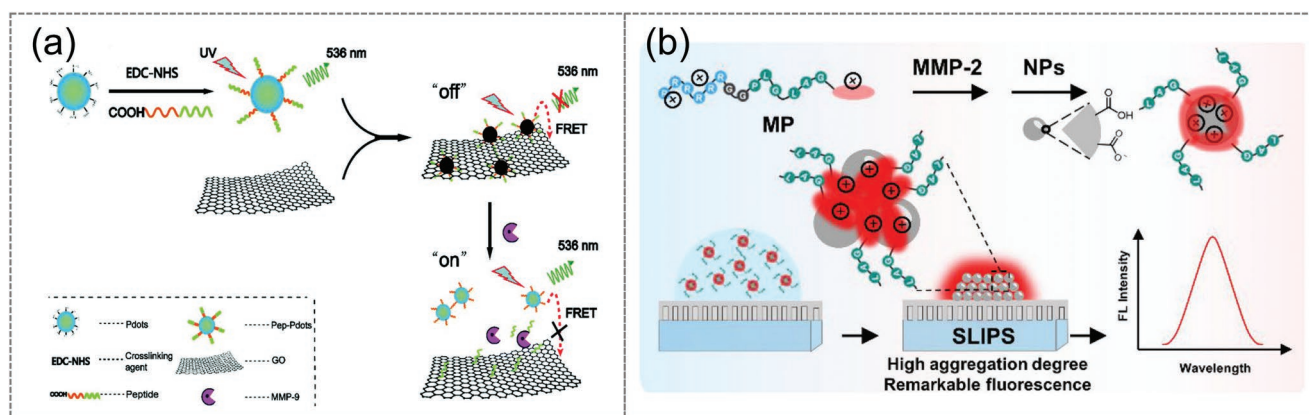


Figure 7. MMPs sensors with outstanding fluorescence signal selected. a) A sensor based on Pep-Pdot nanocomposite for MMP-9 detection. Reproduced with permission.^[75] Copyright 2019, The Royal Society of Chemistry. b) A turn on fluorescent probe sensor (MP/NPs-SLIPS) based on AIE for MMP-2 detection. Reproduced with permission.^[76] Copyright 2021, American Chemical Society.

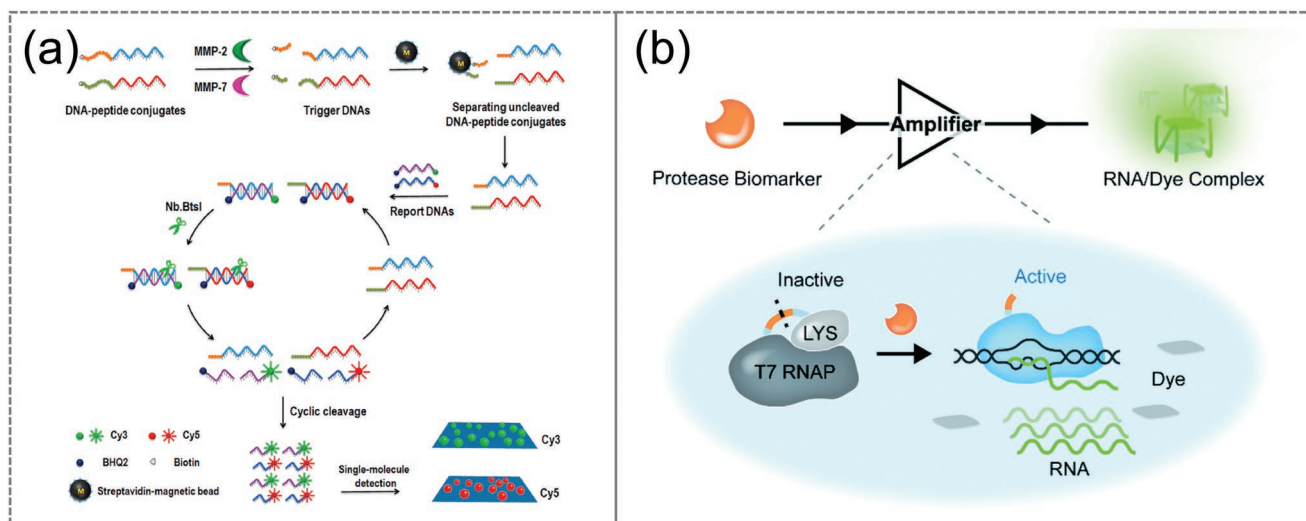


Figure 8. Sensors for MMPs designed using a signaling approach strategy. a) A sensor integrating protease-sensitive cleavage with nicking enzyme-assisted signal amplification for MMP-2 and MMP-7 detection. Reproduced with permission.^[77] Copyright 2020, Elsevier. b) A transcription process-based signal amplifiers sensor for MMP-2 detection. Reproduced with permission.^[78] Copyright 2020, The Royal Society of Chemistry.

In comparison with fluorescence “off-on” sensors, ratiometric fluorescent probes that record the changes of fluorescence signals from two or more different channels are highly desirable for the target analytes detection in complicated biological samples, such as the analysis in tumor microenvironment.^[133,134] In 2022, Chen et al. reported the development of a ratiometric fluorescence nanoprobe for the detection of MMP-7 activity in vitro and in vivo (Figure 9a).^[79] In this nanoprobe, the Rhodamine B (RhB) attached to the surface of MnFe_2O_4 was used as an internal reference probe, and FITC-modified MMP-7 cleavable peptides covalently colinked with MnFe_2O_4 serviced as a reporter for MMP-7 sensing. The emission of FITC was quenched through a FRET process from FITC to MnFe_2O_4 . In the presence of MMP-7, the peptide was specifically cleaved to activate the emission from FITC, and RhB’s emission was retained for the ratiometric analysis. This ratiometric fluorescence sensor was featured with a detection range from 0.1 to 15×10^{-9} M and LoD 0.1×10^{-9} M in vitro, and detection range 5×10^2 – 1×10^4 cells with a LoD 436 cells in in vivo analysis.

For the detection of target analytes in vivo, near-infrared (NIR) fluorescence sensors are preferable because of its high tissue penetration depth. Taking this fact in consideration, Zeng et al. develop a MMP-2 activation ratio NIR fluorescent nanoprobe (SPN-MMP-RGD) for the visualization of MMP-2 activity in vivo in 2021 (Figure 9b).^[80] The SPN-MMP-RGD was designed by combining “always-on” fluorescence of PCP-DTBT ($\lambda_{\text{em}} = 830$ nm) with the NIR fluorophore of Cy5.5 ($\lambda_{\text{em}} = 690$ nm). The MMP-2 triggered activation of Cy5.5 signal allowed the ratiometric fluorescence response ($I_{690/830}$) in vitro and in tumor cells. Interestingly, the cRGD ligand conjugation promoted the tumor targeting of this probe for MMP-2 sensing and imaging in subcutaneous MKN45 tumor bearing mice.

The probe that can detect the MMPs at cell membrane is able to monitor their section at subcellular level. Considered the diffusion of MMPs in the extracellular environment after secretion and the effect of their low secretion on sensor performance, Fang et al. designed a membrane-anchored ratiometric

upconversion nanoprobe (UCNPs-Cy3/Pep-QSY7/Ab) for visualization of MMPs secretion in situ (Figure 10).^[81] In this sensor, Anti-EGFR provided specific recognition for tumor cells and ensured a rapid response to MMP-2 at the local secretion site. MMP-2 triggered the cleavage of Pep-QSY7 (quencher) from the nanoprobe to switch on the upconversion luminescence (UCL) at 540 nm. This UCL enabled the luminescence resonance energy transfer (LRET) to restore Cy3’s emission at 580 nm. Using the UCL at 654 nm as an internal reference, this ratiometric luminescence nanoprobe was demonstrated to monitor MMP-2 secretion in situ in MDAMB-231 and MCF-7 cells and was then successfully applied in vivo imaging of MMP-2 secretion in metastatic lymph node.

In addition to the tumors, MMP-9 has been identified as a biomarker of degenerative central nervous system (CNS) and eye disorders. To determine the MMP-9 in eye disorders, Shin et al. combined the MMP-9 sensor with an intraocular lens (IOL) to fabricate a wearable device for noninvasive visual detection of pathological changes in CNS diseases (Figure 11a).^[135] This intraocular lens sensor was developed based on incorporating dabicyl-quenched 5-FAM within diacrylamide-group-modified poly (ethyleneglycol) (PEGDAAm) biocompatible hydrogels. The MMP-9 triggered cleavage of the peptide for restoring 5-FAM’s emission for MMP-9 detection. In another work, Kambe et al. immobilized the FRET based sensor in silk fibroin (SF) hydrogels to detect MMPs’ activity and study biodegradable SF initial immune response of hydrogels (Figure 11b).^[136] The fluorescence response principle of this sensor is that the cleavage of the peptide inhibited the FRET from monomeric Kusabira-Orange (mKO) to monomeric Kate2 (mKate2), thus the fluorescence of mKate2 was decreased. The experiments results showed that the MMPs cleavage the SF network leads to the loosening of the network, which is conducive to the degradation of the overall level of the hydrogel by immune cells.

In 2021, Cai et al. reported a MMP-9-activated optical imaging probe (MMP-P12) for noninvasive, real-time visualization of

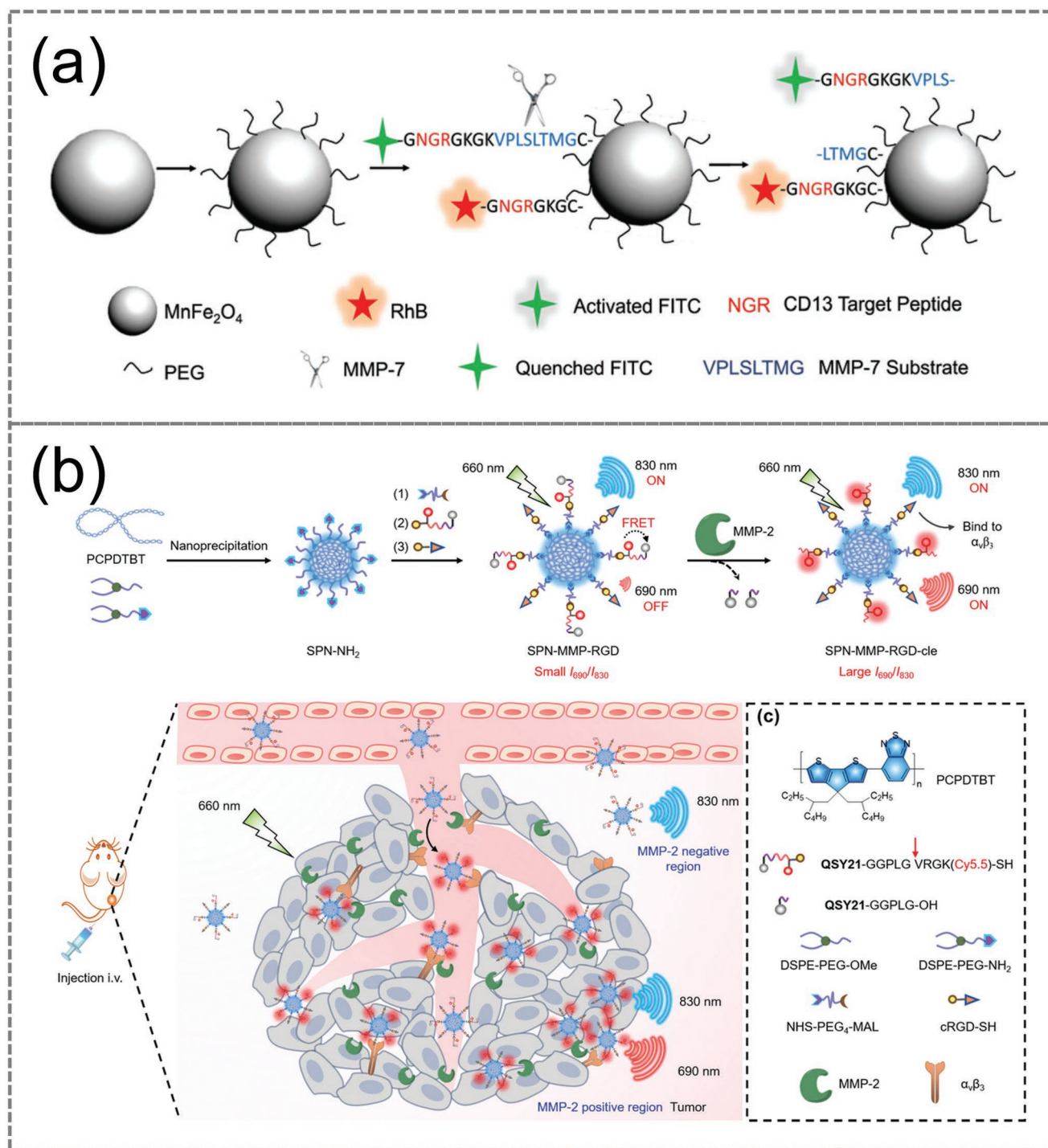


Figure 9. Ratiometric fluorescence based MMPs sensors. a) A ratiometric fluorescent fluorescence nanoprobe based on MnFe_2O_4 for MMP-7 quantitative detection. Reproduced with permission.^[79] Copyright 2022, The Royal Society of Chemistry. b) A ratiometric NIR fluorescent nanoprobe SPN-MMP-RGD for MMP-2 detection. Reproduced with permission.^[80] Copyright 2021, Wiley.

MMP-9 expression and monitoring the therapeutic efficacy of CD28 SA in diabetic stroke (Figure 11c).^[137] In this sensor, the emission of Cy5.5 on a specific size PEG (PEG 12) was quenched by linking of the BHQ-3, and then was switched on after a MMP-9 triggered cleavage of the peptide. Bouquier et al. developed a fluorescent probe based on MMP-2/MMP-9

cleavage to report the activity of MMPs in situ in a model of epilepsy (Figure 11d).^[138] This sensor contains an MMPs-activatable cell-penetrating peptide (ACPP) and a TAMRA fluorophore, allowing fluorescence uptake in cells displaying endogenous gelatinase activity. In a preclinical mouse model of temporal lobe epilepsy (TLE), the probe showed a localized

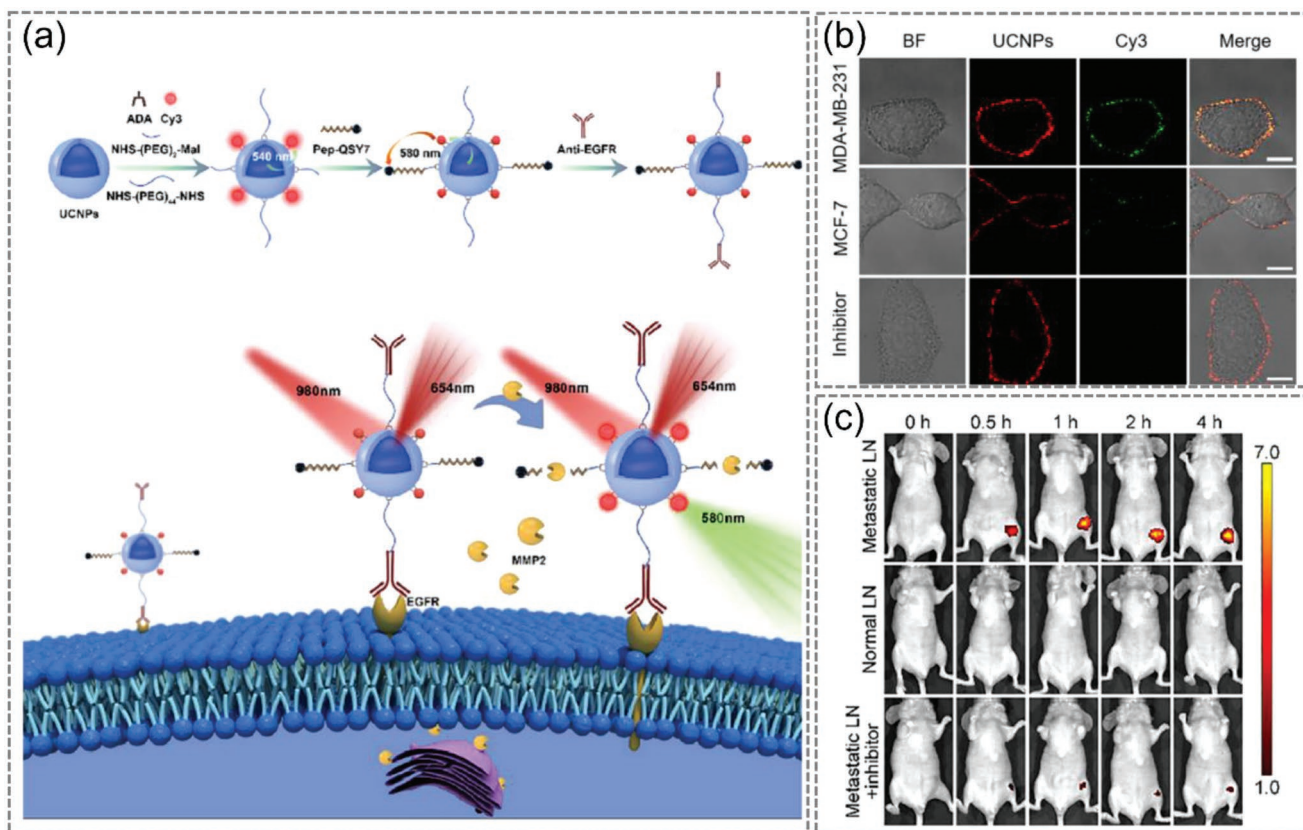


Figure 10. A well-targeted MMP sensor for in vivo application. a) An upconversion nanoprobe UCNPs-Cy3/Pep-QSY7/Ab for in situ monitoring of cell-secreted MMP-2. b) Imaging of upconversion nanoprobe in MDA-MB-231 cells, MCF-7 cells, and inhibitor pretreated MDA-MB-231 cells upon LPS activation. c) Imaging of upconversion nanoprobe in living mice. Reproduced with permission.^[81] Copyright 2021, American Chemical Society.

distribution of MMPs activity. The ability of this sensor to distinguish disease from normal models in practical applications in vivo was then demonstrated.

3.2.2. CL Sensors

CL, the emission light produced as a result of a certain chemical reaction, has been a powerful tool for biosensing and bioimaging research. Since no external excitation light source is required for CL imaging, the interference of autofluorescence is limited, giving it a considerable advantage over fluorescence in terms of signal-to-background ratio.^[139] Among the known chemiluminescent compounds, the triggerable phenoxy-dioxetanes of which the light emission is not activated by oxidation but by phenolate formation following deprotection of phenols are of the highest value for bioimaging. In 2019, Hananya et al. developed a chemiluminescence resonance energy transfer (CRET)-based sensor for the detection of MMP-2 (Figure 12a).^[82] Similar to the FRET principle, in this system the phenoxy-dioxetane luminophore (donor) was conjugated to the quencher (acceptor, 4-(4-nitrophenylazo)aniline) by a MMP-2 cleavable linker. Before enzymatic lysis, the light emission was quenched by nearby receptors through CRET. After the protease hydrolyzed connector, the quencher was detached from the light mass and the luminescence was 160-fold increased. This CL

sensor was then used for MMP-2 activity detection in cancer cells, displaying higher S/N ratio than fluorescent sensors due to the lower background signals.

3.2.3. PA Sensors

The PA effect refers to the phenomenon in which acoustic waves are generated upon irradiation of a simple with pulsed laser. When a medium is irradiated with light, the internal temperature of the medium is changed as a result of the light absorption, which causes the changes in the structure and volume of certain regions in the medium, leading to the generation of acoustic waves. Photoacoustic imaging (PAI) is a new noninvasive and nonionizing biomedical imaging method developed in recent years that combines the advantages of high selectivity in pure optical imaging and deep penetration in pure ultrasound imaging, has ability to obtain high-resolution and high-contrast tissue images, avoiding the influence of light scattering in principle, and realizing deep in vivo tissue imaging.^[140]

PA-based sensors for MMPs have begun to gain attention over the years.^[83,141,142] For example, Yin et al. described a ratiometric small-molecule-based probe for the imaging of MMP-2 activity in tumor-bearing mice in 2019 (Figure 12b).^[83] The probe was developed by linking the NIR fluorophore

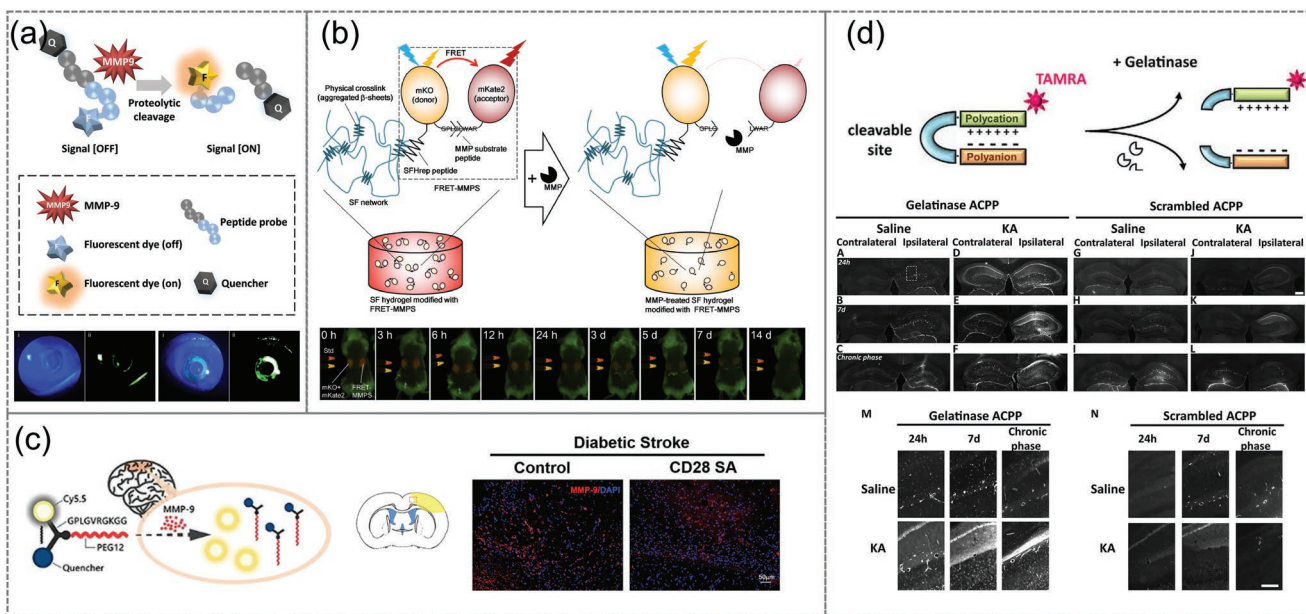


Figure 11. MMP sensors associated with specific problems. a) A FRET-based MMP sensor and its in vivo monitoring ability using fluorogenic IOL. Reproduced with permission.^[135] Copyright 2020, Elsevier. b) A FRET-based MMP sensor-immobilized silk fibroin hydrogel and the fluorescent spectral analysis of the silk fibroin hydrogel modified with FRET-MMPs in vivo. Reproduced with permission.^[136] Copyright 2021, Elsevier. c) A MMP-activatable probe (MMP-P12) which proved CD28 SA treatment can reduce the expression of MMP-9 in STZ-induced diabetic stroke on day 7 post stroke. Reproduced with permission.^[137] Copyright 2021, The Royal Society of Chemistry. d) A fluorescent probe based on MMP-2/MMP-9 cleavage which can report the activity of MMPs in situ in a model of epilepsy. Reproduced with permission.^[138] Copyright 2020, Frontiers Media.

Cy5.5 and the fluorescence quencher QSY21 via a cleavable peptide. Since the probe was composed of hydrophilic Cy5.5 and hydrophobic QSY21 groups, the amphiphilic molecule could spontaneously self-assemble into uniform nanoparticles in aqueous solution. In the absence of MMP-2, fluorescence was quenched due to the FRET principle, and PA signals at 680 and 730 nm were obtained. As a result of the

MMP-2 cleavage of the peptide, high fluorescence signal was observed. A linear decrease in the PA signal at 680 nm was observed while the PA signal at 730 nm remained due to the changes of the aggregation state, allowing for ratiometric PA detection and imaging of MMP-2. This probe was then used for fluorescence and PA imaging of 4T1 tumors in a mice model.

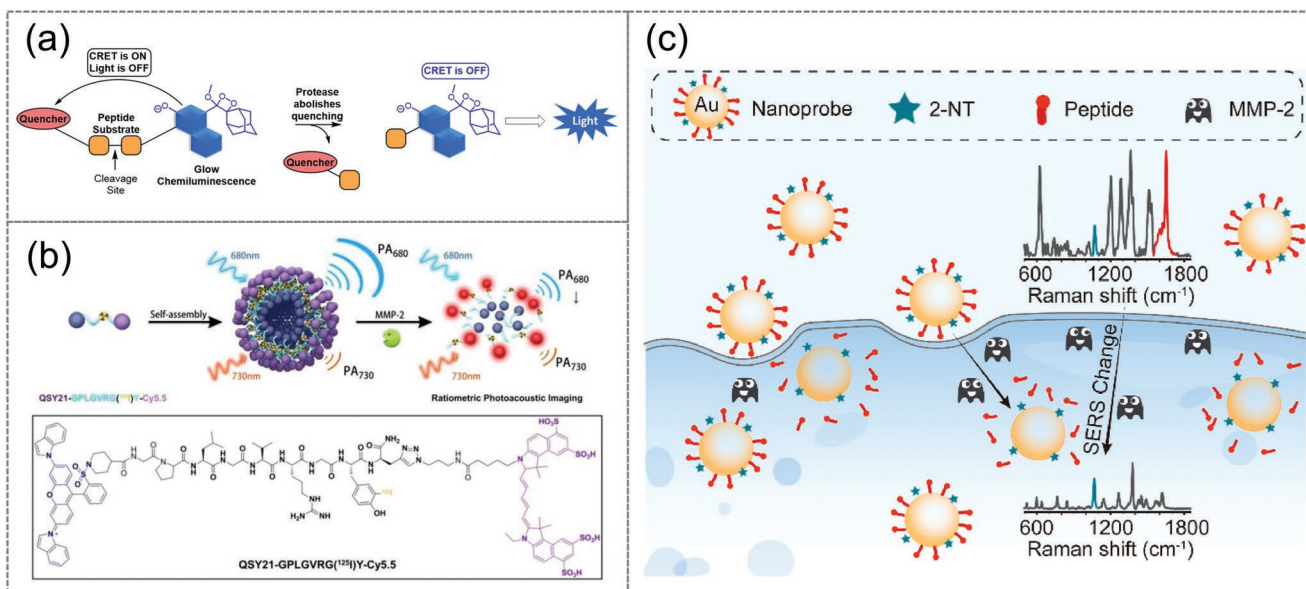


Figure 12. a) A CRET-based sensor for MMP-2 detection.^[82] Copyright 2019, Wiley. b) A ratiometric small-molecule-based PA probe for imaging of MMP-2. Reproduced with permission.^[83] Copyright 2021, Elsevier. c) A ratiometric SERS nanoprobe for MMP-2 imaging. Reproduced with permission.^[84] Copyright 2022, Elsevier.

In another example, Miki et al. described the preparation of the naphthalocyanine (MNC) based PA probe for imaging of MMP-2 in tumor in 2021.^[143] The probe (PEG-peptide-MNC conjugate) was designed by linking the MNC with PEGylated peptide substrate. The PEG-peptide-MNC conjugate assembled to nanosphere in water, producing PA signal at 680 and 760 nm. After the cleavage of the peptide to release of the PEG moiety, the aggregation of MNC was obtained, resulting in 3–5 enhancement of the PA signals. The probe was then used for PAI of MMP-2 in HT-1080 tumor-bearing mice.

3.2.4. SERS Sensors

SERS effect means that in the excitation region, in some specially prepared metal conductor surfaces or sols, the Raman scattering signal of adsorbed molecules is stronger than ordinary Raman scattering due to the enhancement of the electromagnetic field on or near the surface of the sample.^[144] SERS is a fast and sensitive spectroscopic analysis tool with negligible autofluorescence and resistance to photobleaching and quenching, which enables label-free identification and detection of different molecules, and thus this technique has been widely used in bioassay.^[145] Although several SERS-based sensing platforms have been developed for the detection of MMPs in recent years, in situ monitoring of these enzymes in cells by SERS remains a challenge, not to mention the detection of cancer cell subtypes by quantitative SERS imaging. In 2022, Zhong et al. reported a sensitive ratiometric SERS nanoprobe for MMP-2 detection. This nanoprobe consists of three parts, including plasmonic-active gold nanoparticles as the SERS-enhancing matrix, Raman dye RhB-labeled substrate peptide as the specific MMP-2 recognizer, and 2-naphthalenethiol (2-NT) as an internal standard (Figure 12c).^[84] Cleavage of the MMP-2-responsive peptide from the nanoprobe surface resulted in a reduction or even disappearance of the SERS emission of RhB. Finally, the nanoprobe achieved the distinction between normal breast cells and tumor cells, and two different breast cancer cell subtypes.

3.3. Other Sensors

In addition to the electrochemical and optical sensors, other techniques, such as MS and MRI have also been explored for the development of sensors for MMPs detection and imaging, which are briefly highlighted in this section.

3.3.1. MS Sensors

MS is an analytical method that measures the mass-to-charge ratio of ions. MS approaches are exceptionally suitable for clinical analysis due to its high throughput, high sensitivity, and reliable qualitative and quantitative capabilities.^[146] In recent years, researchers have also tried to apply MS to the detection of MMPs.^[147,148] For example, matrix-assisted laser desorption/ionization mass spectrometry (MALDI MS) is suitable for the detection of macromolecules with high sensitivity and

resolution, such as proteins with molecular weights less than 20 kDa. The MMP-2 protein has a molecular weight of 72 kDa, posing a challenge for MALDI spatial detection. To address this challenge, Yu et al. developed a specific sensor for spatial detection of MMP-2 in tissues using MALDI MS (Figure 13a).^[85] The sensor is a peptide containing MMP-2 enzyme cleavage sequence. The peptide has a chlorine atom on the Tyr of the peptide end, which make it has ability to provide two isotopes to improve the detection accuracy. The peptide sensor showed m/z 852 and 854, while the MMP-2 digested segment showed m/z 534 and 536. This method has been successfully applied to the detection of MMP-2 expression and localization sites in colon cancer and normal tissues.

In another example, Hu et al. reported the development of a mass spectrometric biosensing strategy for multiplex detection the activity of MMP-2 and MMP-7 (Figure 13b).^[86] The sensor was developed by coating the nickel-nitrilotriacetic acid-modified magnetic beads (Ni-NTA MBs) with MMP-specific peptide-isobaric tags for relative and absolute quantification (iTRAQ) conjugates through the specific binding between Ni-NTA and hexahistidine tag. In this sensor, the iTRAQ 114 and iTRAQ 117 were used for MMP-2 and MMP-7 detection, respectively, and iTRAQ 115 served as the control. The MMPs-mediated cleavage of the peptide released the iTRAQs and corresponding concentrations were analyzed by UPLC-MS/MS. This sensor showed detection range 0.2–100 and 0.5–400 ng mL⁻¹ with LoD 0.0064 and 0.17 ng mL⁻¹ for MMP-2 and MMP-7 detection, respectively.

3.3.2. MRI Sensors

MRI is realized by the action of high-frequency magnetic field outside the body, and the signal is generated by radiating energy from the objects to the surrounding environment. Due to the different relaxation times of different objects, the manifestation on the image is the difference between light and dark.^[149] MRI does not rely on external radiation, absorption, and reflection, nor on gamma radiation of radioactive substances in the body but uses the interaction of external magnetic fields and objects to image, which is harmless to the human body. In 2020, Yao et al. designed an MRI sensor for MMP-2 detection in the early-stages of abdominal aortic aneurysms (Figure 13c).^[87] The sensor (MMP-Fe/IONPs) was developed by conjugating peptide substrate on the surface of core/shell Fe/iron oxide nanoparticles (Fe/IONPs). The hydrophilic MMP-Fe/IONPs are responsive to MMPs, forming hydrophobic Fe/IONPs after the MMPs-mediated digestion. As a result of the aggregation of the Fe/IONPs, the T2 signals were changed for MRI detection. This MRI probe was then used for the detection of MMPs activity within the cell wall of abdominal aortic aneurysms (AAA), making it a potential noninvasive method for predicting the risk of AAA rupture.

4. Dual-Mode Signal Sensors

Although single signaling analytical technique, such as above overviewed optical and electrochemical sensor, has been promising for MMPs detection and imaging, it is clear that the single

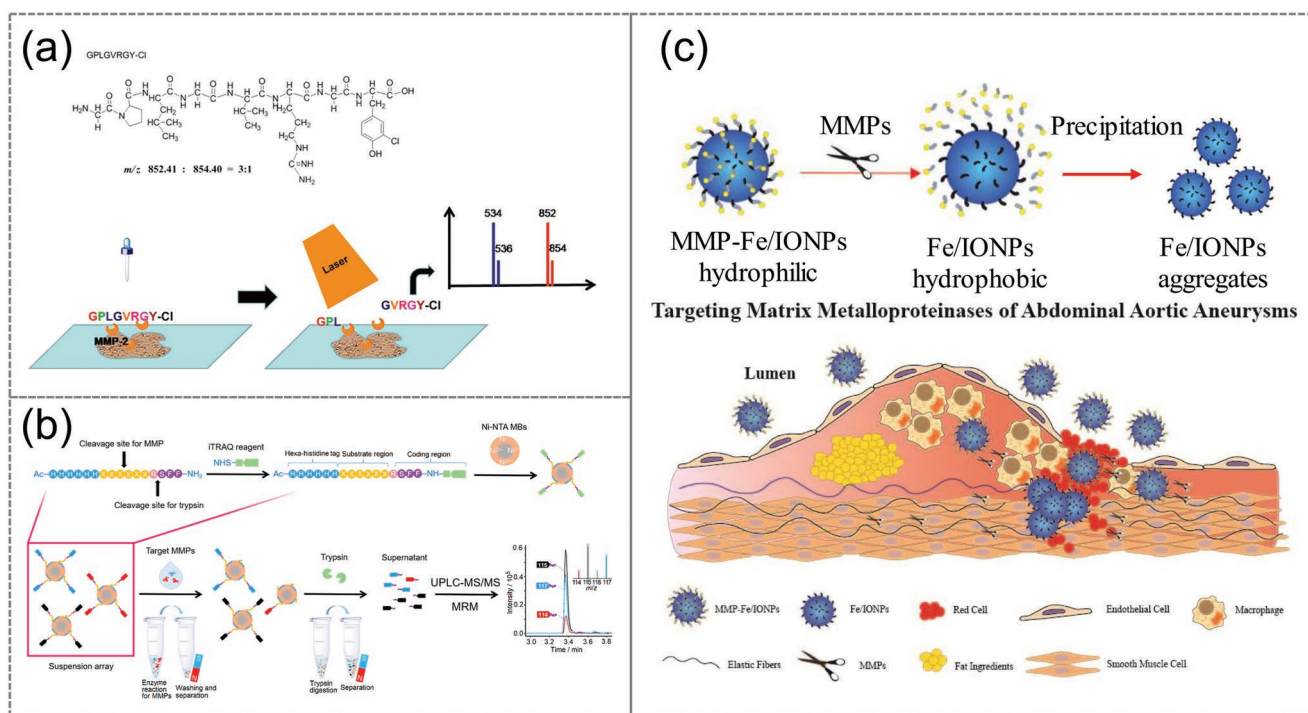


Figure 13. a) A MMP probe based on MALDI imaging mass spectrometry. Reproduced with permission.^[85] Copyright 2021, Frontiers Media. b) A mass spectrometric biosensing strategy for MMP-2 and MMP-7 detection. Reproduced with permission.^[86] Copyright 2022, American Chemical Society. c) An MRI sensor MMP-Fe/IONPs for MMP-2 detection. Reproduced with permission.^[87] Copyright 2020, Elsevier.

signal analysis cannot provide all information about the MMPs' activity in body. As a result, the development of dual-mode sensing platforms has attracted increasing attention in the last three years. A number of dual-mode sensors have been developed for bioassay, including fluorescence/colorimetric,^[150–152] fluorescence/MS,^[153] PAI/MRI,^[154,155] and fluorescence/SERS^[156,157] analyses, and the advances in the development of dual-mode sensors in the last three years are summarized in this section.

Combining the advantages of SERS's high sensitivity and fluorescence's intuitive visualization, Liu et al. developed a fluorescence/SERS dual-mode sensing platform for MMP-2 analysis (Figure 14a).^[88] In this system, the peptide-biotinylated AuNPs was self-assembled with the RB-avidin (RhB-modified avidin) coated magnetic nanoparticles (MNPs) through specific biotin-avidin binding. As a result of the FRET principle, the emission of the nanosensor was quenched. While after the cleavage of the peptide by MMP-2, the fluorescence was switched on, accompanied by the decrease of the RB's SERS intensity at 1647 cm^{-1} . This dual-mode sensor showed high sensitivity (LoD 0.35 ng mL^{-1} for SERS detection and 1.17 ng mL^{-1} for fluorescence detection), and was then used for MMP-2 detection in cells and human serum samples.

Inductively coupled plasma mass spectrometry (ICP-MS), as an element-specific detector, has emerged as a powerful biological quantitative analysis technique. Combing this technique with fluorescence bioassay and imaging, Li et al. designed a simple and reliable MBS-peptide (-FAM)-AuNP bifunctional magnetic microsphere sensor for MMP-2 detection (Figure 14b).^[89] Similarly, the FAM-peptide-biotin coated

magnetic beads was assembled with streptavidin (SA) AuNPs, and thus the emission of FAM was quenched by AuNPs. In this presence of MMP-2, the cleavage of the peptide released the SA-AuNPs and thus switched on the FAM's emission. The AuNPs were also determined by ICP-MS, allowing ICP/MS-fluorescence dual-mode detection of cellular secretion of MMP-2.

5. Dual-Target Detection Platform

The development of sensors for multiple biomarkers detection has been a hot topic in recent years. Generally, in clinical applications, it is hard to make final determination to the diseases' diagnosis and prognosis with information from one biomarker. The development of new sensors for two or more biomarkers detection in parallel, therefore, is essential for biomedical and clinical investigations. In this context, several multiplexed sensors have recently been developed for MMPs and other targeted analytes detection simultaneously, and these sensors are discussed in this section.

In 2020, Zhang et al. reported the development of a multiplexed fluorescence-based sensing system for simultaneous detection of MMPs and ADAMs (a disintegrin and metalloproteinases). The functionalized nanographene oxide (nGO) served as the sensing element in this system (Figure 15a).^[158] This sensing system was able to detect three biomarkers, including MMP-9, ADAM-10, and ADAM-17 in simulated serum samples, demonstrating the potential of this sensing system for the diagnosis of up to five cancer types, including breast cancer, stomach, lung, colorectal, and prostate cancer.

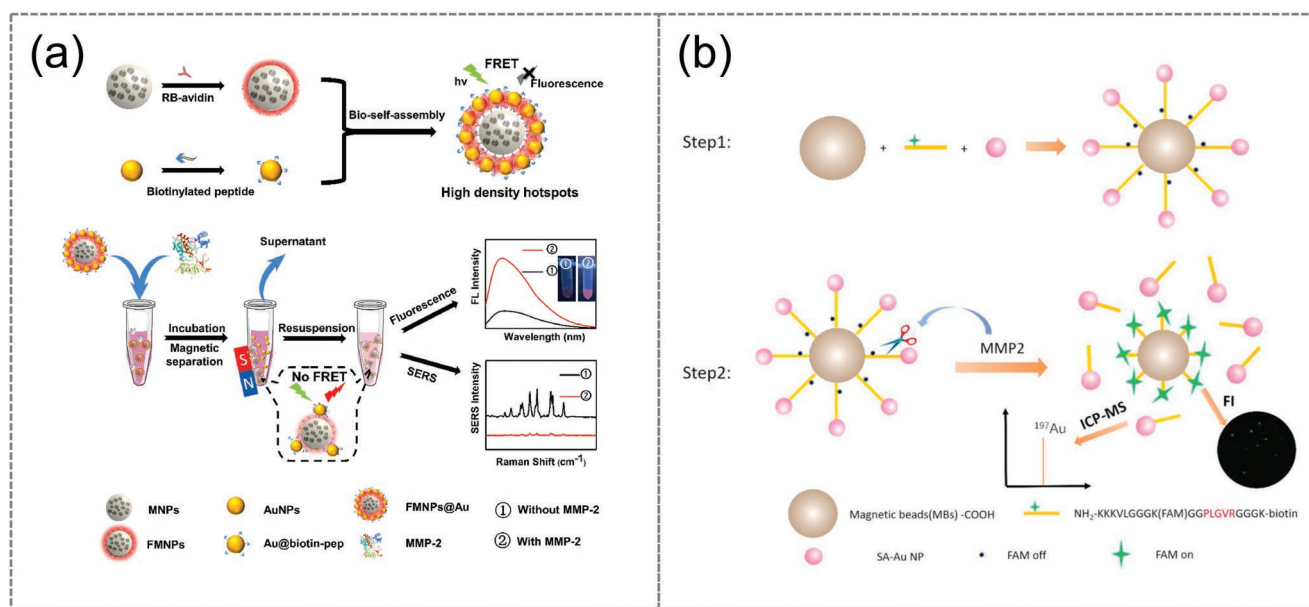


Figure 14. Dual-mode signals MMPs sensors a) A FMNS@Au fluorescence/SERS dual-mode nanosensor for MMP-2 detection. Reproduced with permission.^[88] Copyright 2022, Elsevier. b) An ICP/MS-fluorescence dual-mode sensor based on MBS-peptide (-FAM)-AuNP bifunctional magnetic microsphere for MMP-2 detection. Reproduced with permission.^[89] Copyright 2021, Elsevier.

Urokinase-type plasminogen activator (uPA) is a biomarker that can activate MMP-2 for cancer cell migration and invasion of breast cancer. The overexpression of uPA and MMP-2 has been regarded as the hallmark of malignant tumors in clinical practice. To detect these two biomarkers simultaneously in living cells in real time, Zhan et al. designed a gold-selenium (Au-Se)-based fluorescent nanoprobe by linking rhodamine B (RhB) and fluorescein isothiocyanate (FITC) on Au-Se-modified gold nanoparticles via peptides that can be specifically cleaved by uPA and MMP-2, respectively (Figure 15b).^[159] The nanoprobe showed specific fluorescence signals upon sensing of uPA and MMP-2. Compared with Au-S nanoprobe, Au-Se nanoprobe has better resistance to glutathione (GSH) interference, enhancing the reliability of imaging result.

Considering that elevated intraocular pressure (IOP) and MMP-9 are biomarkers of glaucoma, while elevated IOP has been found to induce MMP-9 activation, ultimately leading to retinal dysfunction. Ye et al. report an optical-based dual-function contact lens sensor for IOP monitoring and MMP-9 detection, enabling real-time and noninvasive diagnosis of glaucoma by integrating biosensors into contact lenses (Figure 15c).^[160] Based on the inverse opal structure, color changes were observed to detect IOP, and MMP-9 was continuously monitored by SERS signal. The LoD of this sensing system to MMP-9 in tears reaches $1.29 \mu\text{g mL}^{-1}$.

In an early research, Gao et al. constructed a protease activation ratiometric fluorescence probe for both pH and MMP-9 detection in the gastric tumor cells and in vivo tumors.^[161] In a following research, the same group developed another fluorescent nanoprobe using a pH-sensitive dye and biocompatible ferric oxide nanoparticles for pH and MMP-9. Compared with the previous probe, Cy5.5 in the system served as an internal reference for the visualization of ratiometric fluorescence responses in vitro and in vivo.^[162] In 2022, Rainu et al. used

pH-responsive carbon nanoparticles modified with the MMP-9 sensitive peptide sequence to combine low pH detection and upregulated MMP detection to delineate malignant tumor areas and normal tissues.^[163] Based on the osteoarthritis (OA) micro-environment marked by MMP-13 overexpression and weak acidity, Chen et al. designed another biocompatible MMP-13/pH response and cartilage targeting ferritin nanocage (CMFn) for OA imaging, followed by adding anti-inflammatory drugs (hydroxychloroquine, HCQ) for treatment (Figure 15d). Ferritin (Fn) nanocages and cy5.5 labeled lysable peptides for pH and MMP-13 response, respectively.^[164]

6. Conclusion

The important role of MMPs in body, especially in the diseases' development drives the studies of the sensors' fabrication targeting these zinc-dependent endopeptidases. In the past three years, a number of sensors have been developed for MMPs detection in vitro and in vivo. In this review, we first highlighted the roles of MMPs in biological system, then summarized the sensors that were developed in the past three years, and focus on the latest progress, research hotspots, and the research development trend. The discussions were mainly based on the sensors developed by MMPs' structure and activity (MMPs cleavable peptide). Among the structure-based sensors, the antibody/antigen binding-based sensors have been widely used in recent years due to the high specificity and sensitivity. Considering the disadvantages such as difficulty in programming antibodies and instability, sensors development based on DNA aptamers, inhibitors, MIPs, etc., have also been developed to make up for these deficiencies. As for cleavage-based enzymatic activity sensors, it can be noted that most of the sensors focus on the detection of MMP-2 and MMP-9. Therefore,

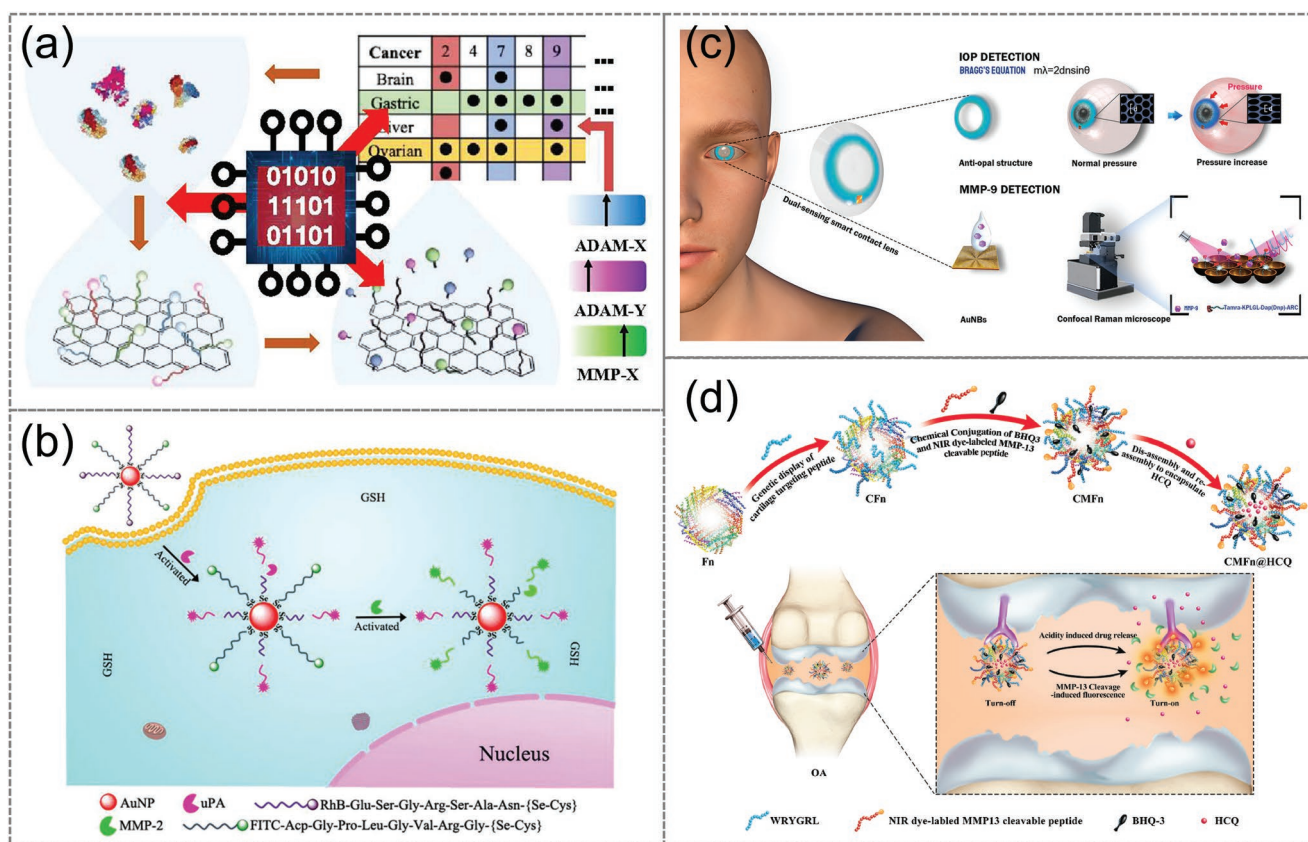


Figure 15. Dual-target detection platform. a) A multiplexed Ngo-COO-Peps biosensor for simultaneous detection of ADAMs and MMPs. Reproduced with permission.^[158] Copyright 2020, American Chemical Society. b) An Au-Se nanoprobe for the simultaneous detection of uPA and MMP-2. Reproduced with permission.^[159] Copyright 2020, The Royal Society of Chemistry. c) A dual-functional contact lens sensor for IOP monitoring and MMP-9 detection. Reproduced with permission.^[160] Copyright 2022, Wiley. d) A CMFn@HCQ-based MMP-13/pH dual-stimulation-activatable nanoprobe for in vivo MMP-13 imaging and therapy in osteoarthritis. Reproduced with permission.^[164] Copyright 2019, Elsevier.

identification of more peptides that are specifically responsive to other MMPs would contribute to the design of new sensors for other MMPs' detection.

In terms of the analytical technique, electrochemical, fluorescence, MS, MRI, PA, CL, and others have been involved in the design of the sensors for MMPs detection. After statistics of the literature in recent years (Table 1), the most widely used techniques are electrochemical and fluorescence sensors, which have high sensitivity, good selectivity, wide linear range, low detection limit, low cost, and easy to use. Nevertheless, the sensing ability of electrochemical sensors is unavoidably limited by the immobilization effect of aptamers, conductivity, and contamination of electrodes by biological samples etc. In clinical applications, the electrode could be contaminated by other biomolecules, resulting in poor sensitivity and selectivity. The interference from the other biomolecules has also been a challenge for the application of fluorescent sensors to detect MMPs in clinical samples. The high background signals from endogenous biomolecules overlap with the fluorescence from the sensors, causing false positive/negative detection results. In addition to electrochemical and fluorescence sensors, ECL, CL, PA, SERS, MS, and MRI sensors have also been developed in recent years for MMPs detection. ECL, CL, and SERS sensors have demonstrated the advantages of high signal-to-noise ratio

for MMPs detection, MS method can provide reliable qualitative and quantitative capabilities. Emerging techniques, such as PA and MRI, offer the opportunity for MMPs detection in vivo as of their high safety and tissue penetration capability. However, the quantification of MMPs using these emerging techniques remains a challenge. Interestingly, dual-mode sensors such as fluorescence/PA, fluorescence/SERS, and fluorescence/MS which bring advantages of individual analytical technique together have been the hot research direction in recent years. The dual-mode sensors have the great potential for MMPs detection in complicated biological samples with high accuracy and precision.

Although a huge number of MMPs sensors with high sensitivity and specificity have been reported, translational research of these sensors as the preclinical and clinical tools and the commercial products has rarely been reported. Some of the publications involved the demonstration of the application of the sensors for clinical samples, such as sera, while it remains far away from the translation of these tools. Therefore, translation of these sensors to clinical studies could be an emerging research direction in the near future.

Overall, over the past three years, huge efforts have been devoted to developing new sensors and to improving their sensing ability for MMPs detection. These efforts include

innovations in the sensing mechanisms (e.g., MIPs, DNA aptamers, and inhibitors-based sensors), further improvements in traditional signals-based sensors (electrochemical and fluorescence sensors), adoption of emerging techniques for sensor's design (e.g., PA, MRI, etc.), developing dual-mode sensors and dual-target sensors, and translational research of these sensors to clinical studies. It is clear that these sensors have been able to detect the activity of MMPs in vitro in biological samples, and the detection of MMPs in situ in vivo could be achieved through integrating conventional sensing mechanisms with new emerging techniques in the next few years. Moreover, besides MMP-2 and MMP-9, the sensors for other MMPs detection in vitro and in vivo would be developed in future. With the advancement of various sensing techniques, we believe that in the near future, more and more MMPs sensors with excellent sensing and imaging capabilities will be developed to facilitate the diagnosis and treatment monitoring of various diseases and promote research about the physiological role of MMPs.

Acknowledgements

The authors gratefully acknowledge the financial support from National Health and Medical Research Council (APP1175808). H.Z. wishes to acknowledge the Ph.D. scholarship support from China Scholarship Council (CSC). Facilities and assistance of the Australian Microscopy & Microanalysis Research Facility at the Centre for Microscopy and Microanalysis (CMM) and Queensland Node of the Australian National Fabrication Facility (ANFF-Q), the University of Queensland, are also acknowledged.

Open access publishing facilitated by The University of Queensland, as part of the Wiley - The University of Queensland agreement via the Council of Australian University Librarians.

Conflict of Interest

The authors declare no conflict of interest.

Keywords

bioassay, matrix metalloproteinases (MMPs), responsive molecule and nanoprobe, sensor

Received: October 21, 2022

Revised: December 13, 2022

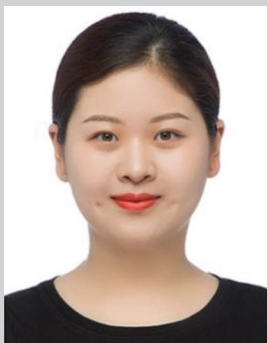
Published online:

- [1] J. Gross, C. M. Lapiere, *Proc. Natl. Acad. Sci. USA* **1962**, 48, 1014.
- [2] H. S. Rasmussen, P. P. McCann, *Pharmacol. Ther.* **1997**, 75, 69.
- [3] M. Egeblad, Z. Werb, *Nat. Rev. Cancer* **2002**, 2, 161.
- [4] H. Nagase, R. Visse, G. Murphy, *Cardiovasc. Res.* **2006**, 69, 562.
- [5] B. Cauwe, G. Opdenakker, *Crit. Rev. Biochem. Mol. Biol.* **2010**, 45, 351.
- [6] T. Feng, H. Tong, Z. Ming, L. Deng, J. Liu, J. Wu, Z. Chen, Y. Yan, J. Dai, *Antiviral Res.* **2022**, 206, 105388.
- [7] Y. Li, X. Zhang, D. He, Z. Ma, K. Xue, H. Li, *Acta Biomater.* **2022**, 145, 372.

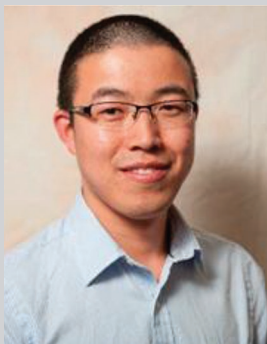
- [8] S. Chakraborty, D. Sampath, M. O. Yu Lin, M. Bilton, C. K. Huang, M. H. Nai, K. Njah, P. A. Goy, C. C. Wang, E. Guccione, C. T. Lim, W. Hong, *Nat. Commun.* **2021**, 12, 6349.
- [9] L. K. Sthanam, T. Roy, S. Patwardhan, A. Shukla, S. Sharma, P. V. Shinde, H. T. Kale, P. C. Shekar, K. Kondabagil, S. Sen, *Biomaterials* **2022**, 280, 121268.
- [10] F. Yang, Q. Chen, M. Yang, E. M. Maguire, X. Yu, S. He, R. Xiao, C. S. Wang, W. An, W. Wu, Y. Zhou, Q. Xiao, L. Zhang, *Cardiovasc. Res.* **2020**, 116, 211.
- [11] W. Lohcharoenkal, L. Wang, T. A. Stueckle, C. Z. Dinu, V. Castranova, Y. Liu, Y. Rojanasakul, *ACS Nano* **2013**, 7, 7711.
- [12] N. Borkakoti, *J. Mol. Med.* **2000**, 78, 261.
- [13] D. E. Kleiner, Jr., W. G. Stetler-Stevenson, *Curr. Opin. Cell Biol.* **1993**, 5, 891.
- [14] M. De Palma, D. Biziato, T. V. Petrova, *Nat. Rev. Cancer* **2017**, 17, 457.
- [15] E. I. Heath, L. B. Grochow, *Drugs* **2000**, 59, 1043.
- [16] Y. Yao, K. Zhao, Z. Yu, H. Ren, L. Zhao, Z. Li, Q. Guo, N. Lu, *J. Exp. Clin. Cancer Res.* **2017**, 36, 103.
- [17] B. C. Sheu, H. C. Lien, H. N. Ho, H. H. Lin, S. N. Chow, S. C. Huang, S. M. Hsu, *Cancer Res.* **2003**, 63, 6537.
- [18] B. Y. Ho, Y. M. Wu, K. J. Chang, T. M. Pan, *Int. J. Biol. Sci.* **2011**, 7, 869.
- [19] F. El-Sharkawi, M. El Sabah, Z. Hassan, H. Khaled, *J. Biomed. Sci.* **2014**, 21, 72.
- [20] P. M. McGowan, M. J. Duffy, *Ann. Oncol.* **2008**, 19, 1566.
- [21] W. Zhou, X. Yu, S. Sun, X. Zhang, W. Yang, J. Zhang, X. Zhang, Z. Jiang, *Biomed. Pharmacother.* **2019**, 118, 109369.
- [22] Q. Yao, L. Kou, Y. Tu, L. Zhu, *Trends Pharmacol. Sci.* **2018**, 39, 766.
- [23] S. Momi, E. Falcinelli, E. Petito, G. C. Taranta, A. Ossoli, P. Gresele, *Eur. Heart J.* **2022**, 43, 504.
- [24] E. A. Goncharova, T. V. Kudryashova, G. Maroli, S. S. Pullamsetti, *Am. J. Respir. Crit. Care Med.* **2021**, 204, 1361.
- [25] E. E. Creemers, J. P. Cleutjens, J. F. Smits, M. J. Daemen, *Circ. Res.* **2001**, 89, 201.
- [26] C. Zhong, J. Yang, T. Xu, T. Xu, Y. Peng, A. Wang, J. Wang, H. Peng, Q. Li, Z. Ju, D. Geng, Y. Zhang, J. He, *Neurology* **2017**, 89, 805.
- [27] S. T. Nikkari, K. D. O'Brien, M. Ferguson, T. Hatsukami, H. G. Welgus, C. E. Alpers, A. W. Clowes, *Circulation* **1995**, 92, 1393.
- [28] A. Page-McCaw, A. J. Ewald, Z. Werb, *Nat. Rev. Mol. Cell Biol.* **2007**, 8, 221.
- [29] B. Chelluboina, K. R. Nalamolu, J. D. Klopfenstein, D. M. Pinson, D. Z. Wang, R. Vemuganti, K. K. Veeravalli, *Mol. Neurobiol.* **2018**, 55, 1405.
- [30] G. A. Rosenberg, *Glia* **2002**, 39, 279.
- [31] V. W. Yong, C. Power, P. Forsyth, D. R. Edwards, *Nat. Rev. Neurosci.* **2001**, 2, 502.
- [32] M. J. Hannocks, X. Zhang, H. Gerwien, A. Chashchina, M. Burmeister, E. Korpos, J. Song, L. Sorokin, *Matrix Biol.* **2019**, 75, 102.
- [33] Y. A. Ghouri, V. Tahan, B. Shen, *World J. Gastroenterol.* **2020**, 26, 3998.
- [34] S. Coward, F. Clement, T. Williamson, G. Hazlewood, S. Ng, S. Heitman, C. Seow, R. Panaccione, S. Ghosh, G. G. Kaplan, *Off. J. Am. Coll. Gastroenterol.* **2015**, 110, S829.
- [35] A. Dufour, C. M. Overall, *Subtracting matrix out of the equation: new key roles of matrix metalloproteinases in immunity and disease. Matrix Metalloproteinase Biology*, Wiley, HOBOKEN, NJ, USA, **2015**.
- [36] M. Majster, R. Lira-Junior, C. M. Höög, S. Almer, E. A. Boström, *Inflammatory Bowel Dis.* **2020**, 26, 1588.
- [37] M. E. Ryan, L. M. Golub, *Periodontol.* **2000** **2000**, 24, 226.
- [38] D. R. Close, *Ann. Rheum. Dis.* **2001**, 60, iii62.
- [39] M. Roderfeld, *Matrix Biol.* **2018**, 68, 452.

- [40] S. Takahashi, M. Ishii, H. Namkoong, A. E. Hegab, T. Asami, K. Yagi, M. Sasaki, M. Haraguchi, M. Sato, N. Kameyama, T. Asakura, S. Suzuki, M. Tasaka, S. Iwata, N. Hasegawa, T. Betsuyaku, *J. Infect. Dis.* **2016**, *213*, 1018.
- [41] P. D. Solan, K. E. Dunsmore, A. G. Denenberg, K. Odoms, B. Zingarelli, H. R. Wong, *Crit. Care Med.* **2012**, *40*, 379.
- [42] J. H. Cox, A. E. Starr, R. Kappelhoff, R. Yan, C. R. Roberts, C. M. Overall, *Arthritis Rheum.* **2010**, *62*, 3645.
- [43] C. L. Bellac, A. Dufour, M. J. Krisinger, A. Loonchanta, A. E. Starr, U. Auf dem Keller, P. F. Lange, V. Goebeler, R. Kappelhoff, G. S. Butler, L. D. Burtnick, E. M. Conway, C. R. Roberts, C. M. Overall, *Cell Rep.* **2014**, *9*, 618.
- [44] Y. C. Chuang, W. T. Huang, P. H. Chiang, M. C. Tang, C. S. Lin, *Biosens. Bioelectron.* **2012**, *32*, 24.
- [45] F. Vadillo-Ortega, D. W. Sadowsky, G. J. Haluska, C. Hernandez-Guerrero, R. Guevara-Silva, M. G. Gravett, M. J. Novy, *Am. J. Obstet. Gynecol.* **2002**, *186*, 128.
- [46] B. Noack, T. Kipping, T. Tervahartiala, T. Sorsa, T. Hoffmann, K. Lorenz, *J. Periodontal Res.* **2017**, *52*, 824.
- [47] D. Wang, Y. Yuan, Y. Zheng, Y. Chai, R. Yuan, *Chem. Commun.* **2016**, *52*, 5943.
- [48] B. Arévalo, A. Ben Hassine, A. Valverde, V. Serafin, A. Montero-Calle, N. Raouafi, J. Camps, M. Arenas, R. Barderas, P. Yáñez-Sedeño, S. Campuzano, J. M. Pingarrón, *Talanta* **2021**, *225*, 122054.
- [49] F. Ma, J. Yan, L. Sun, Y. Chen, *Talanta* **2019**, *205*, 120142.
- [50] C. Chi, Q. Zhang, Y. Mao, D. Kou, J. Qiu, J. Ye, J. Wang, Z. Wang, Y. Du, J. Tian, *Sci. Rep.* **2015**, *5*, 14197.
- [51] H. Lee, Y. P. Kim, *BMB Rep.* **2015**, *48*, 313.
- [52] B. B. Hu, P. Y. Li, X. X. Yang, Y. F. Fan, C. F. Shan, P. R. Su, J. Cao, B. Cheng, W. S. Liu, Y. Tang, *ACS Appl. Bio Mater.* **2019**, *2*, 2978.
- [53] R. Li, Y. Li, M. Mu, B. Yang, X. Chen, W. Y. W. Lee, Y. Ke, W. H. Yung, B. Z. Tang, L. Bian, *ACS Appl. Mater. Interfaces* **2021**, *13*, 11609.
- [54] Q. Wu, K. Wang, X. Wang, G. Liang, J. Li, *J. Mater. Chem. B* **2020**, *8*, 3016.
- [55] K. Wang, Q. Wu, X. Wang, G. Liang, A. Yang, J. Li, *Nanoscale* **2020**, *12*, 10106.
- [56] T. Gong, K. V. Kong, D. Goh, M. Olivo, K. T. Yong, *Biomed. Opt. Express* **2015**, *6*, 2076.
- [57] A. Kirchhain, N. Poma, P. Salvo, L. Tedeschi, B. Melai, F. Vivaldi, A. Bonini, M. Franzini, L. Caponi, A. Tavanti, F. Di Francesco, *Trends Anal. Chem.* **2019**, *110*, 35.
- [58] Z. Lei, M. Jian, X. Li, J. Wei, X. Meng, Z. Wang, *J. Mater. Chem. B* **2020**, *8*, 3261.
- [59] X. Liu, L. Y. Lin, F. Y. Tseng, Y. C. Tan, J. Li, L. Feng, L. Song, C. F. Lai, X. Li, J. H. He, R. Sakthivel, R. J. Chung, *Analyst* **2021**, *146*, 4066.
- [60] M. K. Nisiewicz, A. Kowalczyk, M. Sikorska, A. Kasprzak, M. Bamburowicz-Klimkowska, M. Koszytkowska-Stawińska, A. M. Nowicka, *Talanta* **2022**, *247*, 123600.
- [61] L. Huang, J. Wang, Q. Wang, D. Tang, Y. Lin, *Mikrochim. Acta* **2020**, *187*, 563.
- [62] B. Johannsen, M. Karpíšek, D. Baumgartner, V. Klein, N. Bostanci, N. Paust, S. M. Früh, R. Zengerle, K. Mitsakakis, *Anal. Chim. Acta* **2021**, *1153*, 338280.
- [63] M. K. Nisiewicz, A. Gajda, A. Kowalczyk, A. Cupriak, A. Kasprzak, M. Bamburowicz-Klimkowska, I. P. Grudzinski, A. M. Nowicka, *Anal. Chim. Acta* **2022**, *1191*, 339290.
- [64] J. J. Taylor, K. M. Jaedicke, R. C. van de Merwe, S. M. Bissett, N. Landsdowne, K. M. Whall, K. Pickering, V. Thornton, V. Lawson, H. Yatsuda, T. Kogai, D. Shah, D. Athey, P. M. Preshaw, *Sci. Rep.* **2019**, *9*, 11034.
- [65] X. A. Yu, Y. Hu, Y. Zhang, R. Zhang, X. Bai, L. Gu, H. Gao, R. Li, J. Tian, B. Y. Yu, *ACS Sens.* **2020**, *5*, 1119.
- [66] J. Kim, A. M. Yu, K. P. Kubelick, S. Y. Emelianov, *J. Photoacoust.* **2022**, *25*, 100307.
- [67] K. Gona, J. Toczek, Y. Ye, N. Sanzida, A. Golbazi, P. Boodagh, M. Salarian, J. J. Jung, S. Rajendran, G. Kukreja, T. L. Wu, L. Devel, M. M. Sadeghi, *J. Med. Chem.* **2020**, *63*, 15037.
- [68] K. Bartold, Z. Iskierko, P. Borowicz, K. Noworyta, C. Y. Lin, J. Kalecki, P. S. Sharma, H. Y. Lin, W. Kutner, *Biosens. Bioelectron.* **2022**, *208*, 114203.
- [69] H. Wang, Z. Ma, H. Han, *Bioelectrochemistry* **2019**, *130*, 107324.
- [70] S. Duan, J. Peng, H. Cheng, W. Li, R. Jia, J. Liu, X. He, K. Wang, *Talanta* **2021**, *231*, 122418.
- [71] L. Wang, H. Li, L. Shi, L. Li, F. Jia, T. Gao, G. Li, *Biosens. Bioelectron.* **2022**, *195*, 113671.
- [72] Q. Hu, L. Su, Y. Mao, S. Gan, Y. Bao, D. Qin, W. Wang, Y. Zhang, L. Niu, *Biosens. Bioelectron.* **2021**, *178*, 113010.
- [73] X. Fan, S. Wang, H. Liu, Z. Li, Q. Sun, Y. Wang, X. Fan, *Talanta* **2022**, *236*, 122830.
- [74] Q. Zhang, Z. Chen, Z. Shi, Y. Li, Z. An, X. Li, J. Shan, Y. Lu, Q. Liu, *Biosens. Bioelectron.* **2021**, *193*, 113572.
- [75] Q. Li, Y. Wang, G. Yu, Y. Liu, K. Tang, C. Ding, H. Chen, S. Yu, *Nanoscale* **2019**, *11*, 20903.
- [76] F. Wu, Y. Huang, X. Yang, J. J. Hu, X. Lou, F. Xia, Y. Song, L. Jiang, *Anal. Chem.* **2021**, *93*, 16257.
- [77] Y. Li, W. Liu, Q. Xu, J. Hu, C. Y. Zhang, *Biosens. Bioelectron.* **2020**, *169*, 112647.
- [78] F. Liu, M. Yang, W. Song, X. Luo, R. Tang, Z. Duan, W. Kang, S. Xie, Q. Liu, C. Lei, Y. Huang, Z. Nie, S. Yao, *Chem. Sci.* **2020**, *11*, 2993.
- [79] H. Chen, H. Zhang, Z. Wang, *Analyst* **2022**, *147*, 1581.
- [80] W. Zeng, L. Wu, Y. Sun, Y. Wang, J. Wang, D. Ye, *Small* **2021**, *17*, e2101924.
- [81] Y. Fang, Y. Li, Y. Li, R. He, Y. Zhang, X. Zhang, Y. Liu, H. Ju, *Anal. Chem.* **2021**, *93*, 7258.
- [82] N. Hananya, O. Press, A. Das, A. Scomparin, R. Satchi-Fainaro, I. Sagi, D. Shabat, *Chemistry* **2019**, *25*, 14679.
- [83] L. Yin, H. Sun, H. Zhang, L. He, L. Qiu, J. Lin, H. Xia, Y. Zhang, S. Ji, H. Shi, M. Gao, *J. Am. Chem. Soc.* **2019**, *141*, 3265.
- [84] Q. Zhong, K. Zhang, X. Huang, Y. Lu, J. Zhao, Y. He, B. Liu, *Biosens. Bioelectron.* **2022**, *207*, 114194.
- [85] D. Yu, P. Lai, T. Yan, K. Fang, L. Chen, S. Zhang, *Front. Chem.* **2021**, *9*, 786283.
- [86] J. Hu, F. Liu, Y. Chen, J. Fu, G. Shangguan, H. Ju, *Anal. Chem.* **2022**, *94*, 6380.
- [87] Y. Yao, K. Cheng, Z. Cheng, *Nanomedicine* **2020**, *26*, 102177.
- [88] L. Liu, H. Chu, J. Yang, Y. Sun, P. Ma, D. Song, *Biosens. Bioelectron.* **2022**, *212*, 114389.
- [89] X. Li, B. Chen, M. He, B. Hu, *Anal. Chim. Acta* **2021**, *1161*, 338479.
- [90] E. Gizeli, C. R. Lowe, *Curr. Opin. Biotechnol.* **1996**, *7*, 66.
- [91] C. Wittekind, A. Tannapfel, *Digestion* **1997**, *58*, 79.
- [92] D. Egger, K. Bienz, *Mol. Biotechnol.* **1994**, *1*, 289.
- [93] B. Nilsson, *Curr. Opin. Immunol.* **1989**, *2*, 898.
- [94] C. Lombard, J. Saulnier, J. Wallach, *Biochimie* **2005**, *87*, 265.
- [95] X. C. Cheng, H. Fang, W. F. Xu, *J. Enzyme Inhib. Med. Chem.* **2008**, *23*, 154.
- [96] D. W. Broekaart, A. Bertran, S. Jia, A. Korotkov, O. Senkov, A. Bongaerts, J. D. Mills, J. J. Anink, J. Seco, J. C. Baayen, S. Idema, E. Chabrol, A. J. Becker, W. J. Wadman, T. Tarragó, J. A. Gorter, E. Aronica, R. Prades, A. Dityatev, E. A. van Vliet, *J. Clin. Invest.* **2021**, *131*, e138332.
- [97] Z. Miao, Y. Ding, Y. Bi, M. Chen, X. Cao, F. Wang, *J. Microbiol. Immunol. Infect.* **2021**, *54*, 411.
- [98] S. D. Gan, K. R. Patel, *J. Invest. Dermatol.* **2013**, *133*, e12.
- [99] A. F. M. Jansen, T. Schoffelen, J. Textoris, J. L. Mege, C. P. Bleeker-Rovers, H. I. J. Roest, P. C. Wever, L. A. B. Joosten, M. G. Netea, E. van de Vosse, M. van Deuren, *Clin. Microbiol. Infect.* **2017**, *23*, 487.E7.

- [100] B. B. Kou, L. Zhang, H. Xie, D. Wang, Y. L. Yuan, Y. Q. Chai, R. Yuan, *ACS Appl. Mater. Interfaces* **2016**, *8*, 22869.
- [101] D. S. Shin, Y. Liu, Y. Gao, T. Kwa, Z. Matharu, A. Revzin, *Anal. Chem.* **2013**, *85*, 220.
- [102] F. Ma, Y. Zhu, Y. Chen, J. Liu, X. Zeng, *Talanta* **2019**, *194*, 548.
- [103] Z. Wei, H. Wang, Z. Ma, H. Han, *Nanoscale Res. Lett.* **2018**, *13*, 375.
- [104] A. Biela, M. Watkinson, U. C. Meier, D. Baker, G. Giovannoni, C. R. Becer, S. Krause, *Biosens. Bioelectron.* **2015**, *68*, 660.
- [105] Y. Nie, P. Zhang, H. Wang, Y. Zhuo, Y. Chai, R. Yuan, *Anal. Chem.* **2017**, *89*, 12821.
- [106] H. Park, H. Lee, S. H. Jeong, E. Lee, W. Lee, N. Liu, D. S. Yoon, S. Kim, S. W. Lee, *Anal. Chem.* **2019**, *91*, 8252.
- [107] J. H. Choi, H. Kim, H. S. Kim, S. H. Um, J. W. Choi, B. K. Oh, *J. Biomed. Nanotechnol.* **2013**, *9*, 732.
- [108] A. Khanmohammadi, A. Aghaie, E. Vahedi, A. Qazvini, M. Ghanei, A. Afkhami, A. Hajian, H. Bagheri, *Talanta* **2020**, *206*, 120251.
- [109] F. Mollarasouli, S. Kurbanoglu, S. A. Ozkan, *Biosensors* **2019**, *9*, 86.
- [110] F. Davis, S. P. Higson, *Pediatr. Res.* **2010**, *67*, 476.
- [111] P. Yaiwong, N. Semakul, S. Bamrungsap, J. Jakmunee, K. Ounnunkad, *Bioelectrochemistry* **2021**, *142*, 107944.
- [112] Z. Lu, T. Liu, X. Zhou, Y. Yang, Y. Liu, H. Zhou, S. Wei, Z. Zhai, Y. Wu, F. Sun, Z. Wang, T. Li, J. Hong, *Biosens. Bioelectron.* **2022**, *214*, 114498.
- [113] D. M. Chudakov, M. V. Matz, S. Lukyanov, K. A. Lukyanov, *Physiol. Rev.* **2010**, *90*, 1103.
- [114] P. Teengam, N. Nisab, N. Chuaypen, P. Tangkijvanich, T. Vilaivan, O. Chailapakul, *Biosens. Bioelectron.* **2021**, *189*, 113381.
- [115] D. M. Chen, N. N. Zhang, C. S. Liu, M. Du, *ACS Appl. Mater. Interfaces* **2017**, *9*, 24671.
- [116] M. Chen, C. Grazon, P. Sensharma, T. T. Nguyen, Y. Feng, M. Chern, R. C. Baer, N. Varongchayakul, K. Cook, S. Lecommandoux, C. M. Klapperich, J. E. Galagan, A. M. Dennis, M. W. Grinstaff, *ACS Appl. Mater. Interfaces* **2020**, *12*, 43513.
- [117] M. Amjadi, R. Jalili, *Biosens. Bioelectron.* **2017**, *96*, 121.
- [118] E. Pazos, O. Vázquez, J. L. Mascareñas, M. E. Vázquez, *Chem. Soc. Rev.* **2009**, *38*, 3348.
- [119] X. Zhao, X. Dai, S. Zhao, X. Cui, T. Gong, Z. Song, H. Meng, X. Zhang, B. Yu, *Spectrochim. Acta, Part A* **2021**, *247*, 119038.
- [120] R. E. Wang, Y. Zhang, J. Cai, W. Cai, T. Gao, *Curr. Med. Chem.* **2011**, *18*, 4175.
- [121] J. T. Peterson, *Heart Failure Rev.* **2004**, *9*, 63.
- [122] K. Haupt, P. X. M. Rangel, B. T. S. Bui, *Chem. Rev.* **2020**, *120*, 9554.
- [123] A. Herrera-Chacón, X. Cetó, M. Del Valle, *Anal. Bioanal. Chem.* **2021**, *413*, 6117.
- [124] M. Yuan, Y. Wu, C. Zhao, Z. Chen, L. Su, H. Yang, J. Song, *Theranostics* **2022**, *12*, 1459.
- [125] B. Babamiri, D. Bahari, A. Salimi, *Biosens. Bioelectron.* **2019**, *142*, 111530.
- [126] R. Zhang, J. Yong, J. Yuan, Z. P. Xu, *Coord. Chem. Rev.* **2020**, *408*, 213182.
- [127] H. Feng, J. Liu, A. Qaitoon, Q. Meng, Y. Sultanbawa, Z. Zhang, Z. P. Xu, R. Zhang, *Trends Anal. Chem.* **2021**, *136*, 116199.
- [128] M. Wu, Z. Zhang, J. Yong, P. M. Schenk, D. Tian, Z. P. Xu, R. Zhang, *Top. Curr. Chem.* **2022**, *380*, 29.
- [129] R. Zhang, J. Yuan, *Acc. Chem. Res.* **2020**, *53*, 1316.
- [130] Y. Hong, J. W. Lam, B. Z. Tang, *Chem. Soc. Rev.* **2011**, *40*, 5361.
- [131] X. Cai, B. Liu, *Angew. Chem., Int. Ed. Engl.* **2020**, *59*, 9868.
- [132] X. Luo, J. Zhao, X. Xie, F. Liu, P. Zeng, C. Lei, Z. Nie, *Anal. Chem.* **2020**, *92*, 16314.
- [133] R. Zhang, B. Song, J. Yuan, *Trends Anal. Chem.* **2018**, *99*, 1.
- [134] C. Liu, X. Gao, J. Yuan, R. Zhang, *Trends Anal. Chem.* **2020**, *133*, 116092.
- [135] M. K. Shin, Y. W. Ji, C. E. Moon, H. Lee, B. Kang, W. S. Jinn, J. Ki, B. Mun, M. H. Kim, H. K. Lee, S. Haam, *Biosens. Bioelectron.* **2020**, *162*, 112254.
- [136] Y. Kambe, T. Yamaoka, *Acta Biomater.* **2021**, *130*, 199.
- [137] Y. Cai, S. Leng, Y. Ma, T. Xu, D. Chang, S. Ju, *Biomater. Sci.* **2021**, *9*, 2562.
- [138] N. Bouquier, B. Girard, J. A. Arias, L. Fagni, F. Bertaso, J. Perroy, *Front. Synaptic Neurosci.* **2020**, *12*, 15.
- [139] A. Tiwari, S. J. Dhoble, *Talanta* **2018**, *180*, 1.
- [140] L. Zeng, G. Ma, J. Lin, P. Huang, *Small* **2018**, *14*, 1800782.
- [141] K. Miki, N. Imaizumi, K. Nogita, M. Oe, H. Mu, W. Huo, H. Harada, K. Ohe, *Bioconjugate Chem.* **2021**, *32*, 1773.
- [142] H. Qin, Y. Zhao, J. Zhang, X. Pan, S. Yang, D. Xing, *Nanomedicine* **2016**, *12*, 1765.
- [143] K. Miki, N. Imaizumi, K. Nogita, M. Oe, H. Mu, W. Huo, H. Harada, K. Ohe, *Bioconjugate Chem.* **2021**, *32*, 1773.
- [144] J. Perumal, Y. Wang, A. B. E. Attia, U. S. Dinis, M. Olivo, *Nanoscale* **2021**, *13*, 553.
- [145] J. Li, A. Wuethrich, S. Dey, R. E. Lane, A. A. I. Sina, J. Wang, Y. Wang, S. Puttick, K. M. Koo, M. Trau, *Adv. Funct. Mater.* **2020**, *30*, 1909306.
- [146] J. Hu, F. Liu, Y. Chen, G. Shangguan, H. Ju, *ACS Sens.* **2021**, *6*, 3517.
- [147] Y. C. Hsiao, S. Y. Lin, K. Y. Chien, S. F. Chen, C. C. Wu, Y. T. Chang, L. M. Chi, L. J. Chu, W. F. Chiang, C. Y. Chien, K. P. Chang, Y. S. Chang, J. S. Yu, *Anal. Chim. Acta* **2020**, *1100*, 118.
- [148] Y. Wang, D. V. Zagorevski, M. R. Lennartz, D. J. Loegering, J. A. Stenken, *Anal. Chem.* **2009**, *81*, 9961.
- [149] Q. Meng, M. Wu, Z. Shang, Z. Zhang, R. Zhang, *Coord. Chem. Rev.* **2022**, *457*, 214398.
- [150] L. Tang, K. Liang, L. Wang, C. Chen, C. Cai, H. Gong, *Anal. Chem.* **2022**, *94*, 13879.
- [151] Y. Shen, X. Gao, Y. Zhang, H. Chen, Y. Ye, Y. Wu, *J. Hazard. Mater.* **2022**, *439*, 129582.
- [152] T. Pei, Y. He, Y. Wang, G. Song, *Mikrochim. Acta* **2021**, *189*, 7.
- [153] N. Volpi, F. Galeotti, B. Yang, R. J. Linhardt, *Nat. Protoc.* **2014**, *9*, 541.
- [154] N. Ding, K. Sano, K. Kanazaki, Y. Shimizu, H. Watanabe, T. Namita, T. Shiina, M. Ono, H. Saji, *J. Pharm. Sci.* **2020**, *109*, 3153.
- [155] X. Hu, Y. Tang, Y. Hu, F. Lu, X. Lu, Y. Wang, J. Li, Y. Li, Y. Ji, W. Wang, D. Ye, Q. Fan, W. Huang, *Theranostics* **2019**, *9*, 4168.
- [156] N. Hao, Z. Pei, P. Liu, H. Bachman, T. D. Naquin, P. Zhang, J. Zhang, L. Shen, S. Yang, K. Yang, S. Zhao, T. J. Huang, *Small* **2020**, *16*, 2005179.
- [157] X. Niu, H. Chen, Y. Wang, W. Wang, X. Sun, L. Chen, *ACS Appl. Mater. Interfaces* **2014**, *6*, 5152.
- [158] Y. Zhang, X. Chen, S. Yuan, L. Wang, X. Guan, *Anal. Chem.* **2020**, *92*, 15042.
- [159] R. Zhan, X. Li, L. Zang, K. Xu, *Analyst* **2020**, *145*, 1008.
- [160] Y. Ye, Y. Ge, Q. Zhang, M. Yuan, Y. Cai, K. Li, Y. Li, R. Xie, C. Xu, D. Jiang, J. Qu, X. Liu, Y. Wang, *Adv. Sci.* **2022**, *9*, 2104738.
- [161] Y. Hou, J. Zhou, Z. Gao, X. Sun, C. Liu, D. Shangguan, W. Yang, M. Gao, *ACS Nano* **2015**, *9*, 3199.
- [162] T. Ma, Y. Hou, J. Zeng, C. Liu, P. Zhang, L. Jing, D. Shangguan, M. Gao, *J. Am. Chem. Soc.* **2018**, *140*, 211.
- [163] S. Rainu, S. Parameswaran, S. Krishnakumar, N. Singh, *J. Mater. Chem. B* **2022**, *10*, 5388.
- [164] H. Chen, Z. Qin, J. Zhao, Y. He, E. Ren, Y. Zhu, G. Liu, C. Mao, L. Zheng, *Biomaterials* **2019**, *225*, 119520.



Huayue Zhang received her bachelor (2018) and master (2021) from the Tianjin University. She is now a Ph.D. student at the Australian Institute for Bioengineering and Nanotechnology, The University of Queensland (AIBN UQ) under the supervision of Dr. Run Zhang, Prof. Zhi Ping (Gordon) Xu, and Assoc. Prof. Hang Thu Ta. She is interested in developing responsive probes (sensors) for disease biomarkers detection.



Run Zhang is a Senior Research Fellow at the Australian Institute for Bioengineering and Nanotechnology, The University of Queensland (AIBN UQ). He received his Ph.D. in Chemistry from Dalian University of Technology in 2012. He worked at Macquarie University (MQ) as Postdoc (2012) and independent MQ Research Fellow (2013–2015). He joined AIBN UQ in 2016 and received ARC DECRA (2017–2019) and NHMRC Emerging Leadership (2020). He now leads a team of more than ten research higher degree (RHD) students at AIBN UQ, working on the development of responsive molecules/nanomaterials for biosensing and imaging, early disease detection and treatment, and food/agricultural/environmental analysis.